

# Specific types of male infertility are correlated with T cell exhaustion or senescence signatures

Received: 29 February 2024

Accepted: 10 January 2025

Published online: 24 January 2025

 Check for updates

Giada Amodio <sup>1</sup>, Giorgia Giacomini<sup>1</sup>, Luca Boeri<sup>2</sup>, Massimiliano Raffo<sup>3,4</sup>, Simone Cilio <sup>3,5</sup>, Edoardo Pozzi<sup>3,4</sup>, Federico Belladelli<sup>3,4</sup>, Fausto Negri <sup>3,4</sup>, Anna Maria Ferrara<sup>3</sup>, Alessia d'Arma<sup>3</sup>, Francesca Romana Santoni de Sio<sup>1</sup>, Luca Pagliardini<sup>6</sup>, Enrico Papaleo<sup>6</sup>, Eugenio Ventimiglia<sup>3</sup>, Massimo Alfano <sup>3</sup>, Francesco Montorsi<sup>3,4</sup>, Andrea Salonia <sup>3,4,7</sup>  & Silvia Gregori <sup>1,7</sup> 

The association between male infertility and health status has yet to be unraveled. Here, by combining multiparameter phenotyping and scRNA-seq, we delineate the immune status of infertile men both at the semen and systemic levels. We first observe that young infertile men have a pro-inflammatory milieu with increased frequency of myeloid cells and inflammatory mediators in the seminal fluid and the peripheral blood, which are immune alterations typically observed in healthy elderly men. Transcriptomic profiling confirms the upregulation of genes associated with the interferon-gamma and -alpha responses in peripheral blood T cells of infertile men with oligo-asthenoteratozoospermia or non-obstructive azoospermia, with distinct T cell signatures of exhaustion and senescence discriminating the two infertile conditions. These findings provide evidence that subtypes of male infertility are characterized by specific immune signatures and unravel the potential link between infertility and the risk of developing secondary diseases.

Infertility affects up to 15% of couples worldwide<sup>1</sup>. A pure male factor is responsible for about 20% of cases, being a contributing factor in up to 30% of all infertility cases. After a diagnostic work-up, at least one underlying cause of male infertility can be identified in most of the cases<sup>2</sup>. The interest in understanding both causes and consequences of male infertility has steadily grown over the last years, and several findings have contributed to change in the definition of infertility from an epiphenomenon to a disease itself and a clinical proxy of poorer general health status compared to age-matched fertile men<sup>3–5</sup>. Indeed, infertile men are at high risk of premature development of non-malignant and malignant non-communicable diseases (NCDs) in a relatively short time frame<sup>6–8</sup>. Likewise, infertility has also been

associated with high mortality risk, mostly observed in severe infertile individuals<sup>9</sup>.

A comprehensive understanding of the association between male infertility and the overall impoverishment of patients's health is still lacking. From a pathogenetic standpoint, infertile men are depicted as having immature testis, characterized by low testicular volume, an altered hormonal milieu, and paternally imprinted genes, along with immature Sertoli and Leydig cells<sup>10</sup>. Recently, we have shown that the testis of men with idiopathic non-obstructive azoospermia (NOA) displays an altered composition of the extracellular matrix<sup>11</sup>, microbial dysbiosis<sup>12</sup>, and a senescent phenotype of somatic cells combined with a pro-inflammatory profile of

<sup>1</sup>San Raffaele Telethon Institute for Gene Therapy (SR-TIGET), IRCCS Ospedale San Raffaele, Milan, Italy. <sup>2</sup>IRCCS Fondazione Ca' Granda Ospedale Maggiore Policlinico, Department of Urology, Milan, Italy. <sup>3</sup>Division of Experimental Oncology/Unit of Urology; URI; IRCCS Ospedale San Raffaele, Milan, Italy. <sup>4</sup>University Vita-Salute San Raffaele, Milan, Italy. <sup>5</sup>Department of Neurosciences, Reproductive Sciences and Odontostomatology, Urology Unit, University of Naples "Federico II", Naples, Italy. <sup>6</sup>Reproductive Sciences Laboratory, Obstetrics and Gynaecology Unit, IRCCS Ospedale San Raffaele, Milan, Italy. <sup>7</sup>These authors jointly supervised this work: Andrea Salonia, Silvia Gregori.  e-mail: [salonia.andrea@hsr.it](mailto:salonia.andrea@hsr.it); [gregori.silvia@hsr.it](mailto:gregori.silvia@hsr.it)

**Table 1 | Descriptive statistics of the entire cohort of participants**

	FER (n = 33)	OAT (n = 34)	NOA (n = 12)
<b>Semen parameters</b>			
Concentration (10 <sup>6</sup> /ml)	50.4 ± 7.7	4.5 ± 0.7****	N.A.
Progressive motility (%)	41.7 ± 2.1	11.9 ± 1.6****	N.A.
Normal morphology (%)	3.2 ± 0.3	1.2 ± 0.1****	N.A.
<b>Clinical parameters</b>			
Age, years	36.2 ± 1.2	37.9 ± 1.1	36.7 ± 2.1
BMI (kg/m <sup>2</sup> )	25.4 ± 0.5	25.6 ± 0.6	27.5 ± 1.2
Waist circumference (cm)	90.2 ± 1.7	97.2 ± 1.8*	100.4 ± 3.3**
Regular physical activity (%)	42.4	67.6	41.7
Active smokers (%)	46.8	11.8	25
CCI = 0 (%)	91.0	88.3	75.1
CCI = 1 (%)	9.0	8.8	8.3
CCI > 1 (%)	0	2.9	16.6
HBP (%)	6.0	8.8	8.3
Comorbidities (n, type)	2, hypothyroidism	1, Hashimoto	1, CD; 1, T1D
Average testicular volume (ml)	19.3 ± 0.7	17.0 ± 0.8	12.5 ± 1.6**
PSA (ng/ml)	0.76 ± 0.07	0.82 ± 0.1	0.76 ± 0.1
HbA1c (%)	32.8 ± 0.5	32.2 ± 0.5	34.9 ± 2.1
Glycemia (mg/dL)	N.T.	88.7 ± 1.7	90.3 ± 3.1
Albumin (g/L)	N.T.	45.1 ± 1.3	45.6 ± 1.4
<b>Hormonal parameters</b>			
tT (ng/ml)	4.3 ± 0.2	5.2 ± 0.3	4.6 ± 0.5
SHBG (nmol/L)	30.1 ± 1.9	39.5 ± 3.9	30.9 ± 4.1
E2 (pg/ml)	19.7 ± 1.6	23.1 ± 2.1	24.2 ± 2.7
FSH (UI/ml)	4.1 ± 0.4	5.7 ± 0.6 <sup>§</sup>	21.8 ± 4.5****
LH (UI/ml)	4.6 ± 0.3	4.7 ± 0.4 <sup>§§</sup>	10.5 ± 1.7**
TSH (mU/ml)	2.6 ± 0.4	2.1 ± 0.2	1.9 ± 0.3
AMH (ng/ml)	6.1 ± 0.7	7.7 ± 1.0 <sup>§</sup>	4.7 ± 1.7
PTH (pg/ml)	N.T.	46.3 ± 3.1 <sup>§</sup>	36.6 ± 3.5
Inhibin B (pg/ml)	N.T.	176.9 ± 20.9 <sup>§§§</sup>	60.8 ± 18.0
Prolactin (micro IU/L)	16.2 ± 1.5	15.9 ± 5.2	22.3 ± 8.6
VitD3 (ng/ml)	N.T.	23.4 ± 1.5	23.4 ± 2.2

Data are presented as mean ± SEM. For each variable, the Kruskal-Wallis test, in association with Dunn's multiple comparison tests, was used to test the difference between three groups; the two-sided Mann-Whitney test was used to test the difference between two groups. \* $P \leq 0.05$ , \*\* $P \leq 0.01$ , \*\*\* $P \leq 0.001$ , and \*\*\*\* $P \leq 0.0001$  all vs. FER; § $P \leq 0.05$ , §§ $P \leq 0.01$ , and §§§ $P \leq 0.001$  vs. NOA. FER, fertile men; OAT, Oligo-Astheno-Terato spermia patients; NOA, non-obstructive azoospermia patients; N.A., not applicable; N.T., not tested; BMI, Body Mass Index; CCI, Charlson comorbidity index; HBP, high blood pressure; PSA, Prostate-Specific Antigen; HbA1c, glycosylated hemoglobin; tT, total testosterone; SHBG, sex hormone binding globulin; E2, 17 $\beta$ -estradiol; FSH, follicle-stimulating hormone; LH, luteinizing hormone; TSH, thyroid stimulating hormone; AMH, Anti-Müllerian Hormone; PTH, parathyroid hormone; CD, celiac disease; T1D, type 1 diabetes.

macrophages and T cells, and signs of chronic inflammation in the peripheral blood<sup>13</sup>.

Inflammation is a complex biological process in response to harmful stimuli required to eliminate the cause of cell injury with the subsequent induction of tissue repair. This process involves innate and adaptive immune responses, with the first signs of inflammation being the recruitment of monocytes, neutrophils, and macrophages<sup>14,15</sup>, followed by the release of pro-inflammatory mediators<sup>16</sup>. Throughout this

phase, the adaptive immune response sustains the inflammatory process, whilst it thereafter contributes to its resolution through the action of regulatory T and myeloid cells<sup>17,18</sup>. When the inflammation becomes either chronic or dysregulated, it can contribute to the pathogenesis of several diseases<sup>19</sup>. During chronic inflammation, the persistent stimulation of T cells reprograms their phenotype and functions, thus leading them to exhaustion or senescence<sup>20</sup>. T-cell exhaustion is a reversible state associated with progressive loss of cytokine production and cytotoxic activity, along with an increased expression of inhibitory molecules<sup>21</sup>. Conversely, T-cell senescence is associated with permanent cell cycle arrest, changes in gene expression, the ability to secrete a pattern of factors known as senescence-associated secretory phenotype (SASP), and altered cell surface markers<sup>22</sup>. This condition is often associated with aging, but it can also occur prematurely in response to chronic antigen stimulation or other stressors such as oxidative and genotoxic stress and mitochondrial dysfunction<sup>22,23</sup>.

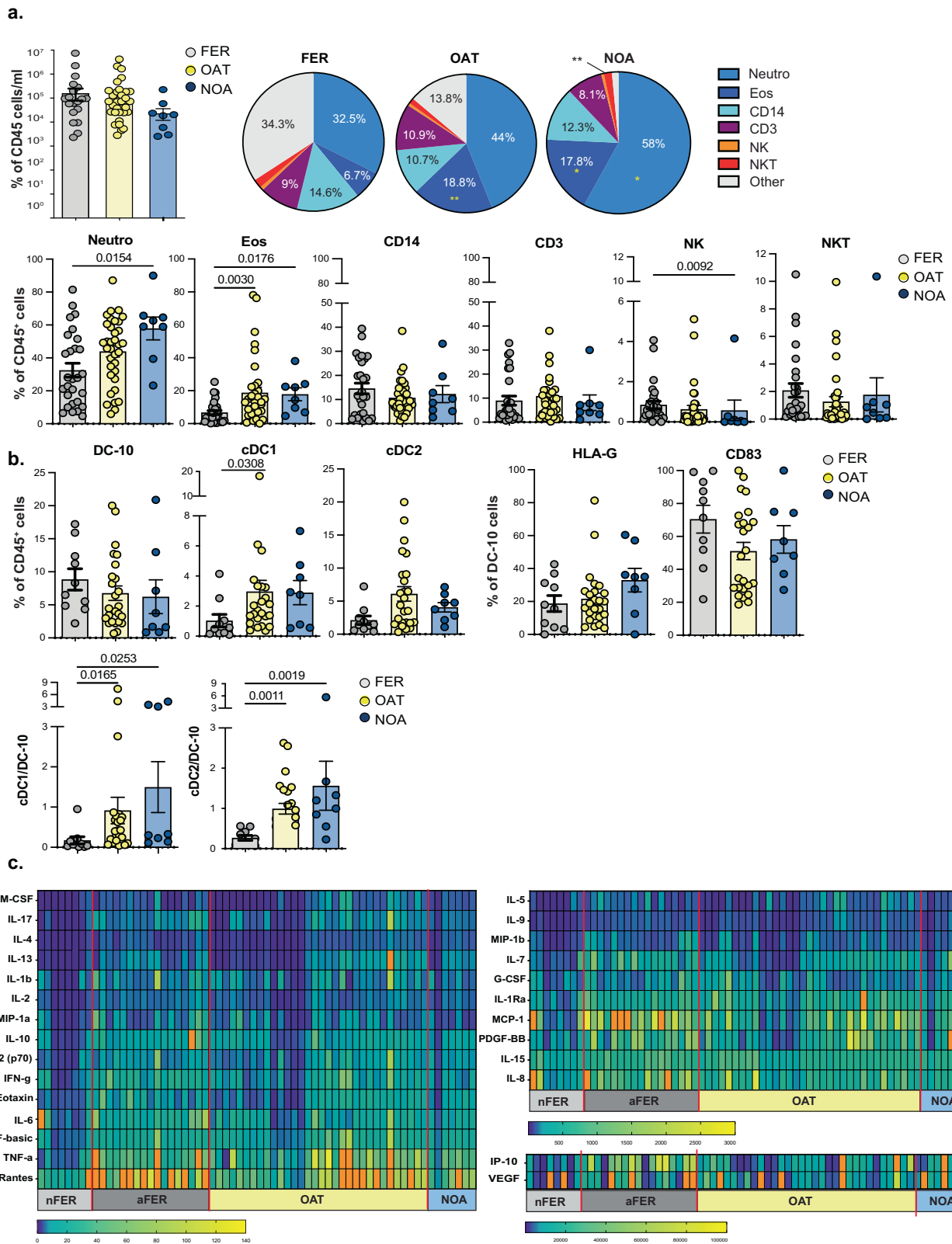
Here, we test the hypothesis that immune deregulation is associated with male infertility and has an impact on patients' overall health status. A thoughtful tissue-specific and systemic analysis of the immune composition of infertile men shows that severe infertile men are characterized by a tissue-specific (e.g., semen) and systemic (e.g., peripheral blood) pro-inflammatory signature associated with an increased proportion of granulocytes and dendritic cells (DC), and a reduced frequency of T cells. Single-cell transcriptome profiling of peripheral blood T cells reveals a signature of exhaustion in infertile patients affected by oligo-astheno-teratozoospermia (OAT) and of senescence in NOA patients. Our findings demonstrate that although infertile men at the time of the analysis are healthy individuals, they show specific immune alterations that can be used to discriminate subtypes of male infertility and sustain previous observations that infertile men are less healthy than age-matched fertile men.

## Results

### Aberrant spermatozoa are associated with a pro-inflammatory environment in the semen

Immune deregulation could be associated with male infertility and has an impact on patients' overall health status. Thus, we investigated the presence and the relative frequency of the major leukocyte populations in the semen of OAT and NOA patients as compared with same-ethnicity, age-matched fertile (FER) controls (Table 1). The overall abundance of hematopoietic CD45<sup>+</sup> cells in semen is comparable among groups, with an absolute count below 10<sup>6</sup> cells/ml (Fig. 1a and Supplementary Fig. 1a), indicating the absence of leuko-cytospermia (WHO laboratory manual for the examination and processing of human semen, 6<sup>th</sup> edition. Geneva: WHO 2021. Licence: CC BY-NC-SA 3.0 IGO). We confirm<sup>24</sup> that granulocytes are the most abundant cell subset in the semen, with the frequency of neutrophils being higher in OAT and NOA compared to FER men, reaching statistical significance in NOA patients (Fig. 1a). The frequency of eosinophils also results significantly higher in OAT and NOA than FER men (Fig. 1a). As expected, CD14<sup>+</sup> cells represent the 20–30% and lymphocytes 10–12% of CD45<sup>+</sup> cells in the semen; moreover, groups do not differ in terms of CD14, CD3, NK, and NKT cell proportions, except for NK cells that are significantly less abundant in NOA compared to FER men (Fig. 1a).

Tolerogenic DC-10 (CD11c<sup>+</sup>CD14<sup>+</sup>CD16<sup>+</sup>CD163<sup>+</sup>CD141<sup>+</sup>), expressing HLA-G and CD83 - two markers associated with their functionality<sup>25–27</sup> - are present at a comparable frequency in the semen of OAT, NOA, and FER men (Fig. 1b and Supplementary Fig. 1b). Conversely, the proportion of classical (c)DC1 (CD14<sup>+</sup>CD11c<sup>+</sup>CD141<sup>+</sup>) is higher in both OAT and NOA compared to FER men, reaching statistical significance in OAT patients. A trend toward an increased frequency of inflammatory cDC2 (CD11c<sup>+</sup>CD1c<sup>+</sup>) in the semen of OAT and NOA compared to FER men is also observed. Although cDC1 and cDC2 in OAT, NOA, and FER men expressed CD83 at similar levels (Supplementary Fig. 2), cDC1/DC-



10 and cDC2/DC-10 ratios are in favor of inflammatory cells and significantly higher in both OAT and NOA as compared with FER men (Fig. 1b). Thus, the semen of OAT and NOA patients is characterized by a higher proportion of pro-inflammatory DC, which are phenotypically similar to those of FER men.

The assessment of cytokine/chemokine content in the semen reveals two groups of FER men characterized by different amounts of

analytes (Fig. 1c). In line with previous studies describing an association between high levels of certain cytokines in the semen and the quality of sperm parameters<sup>28,29</sup>, we detect a high content of almost all cytokines and chemokines analyzed in the sub-group of FER men with impaired semen quality (e.g., containing spermatozoa with one or two alterations, Supplementary Table 1) and we define this group as abnormal FER men (aFER) compared to those with completely normal

**Fig. 1 | Pro-inflammatory environment in the semen of severe infertile patients.** **a–b** The proportion of the major leukocyte subsets, including dendritic cells (DC), was analyzed by multiparametric flow cytometry in the sperm fluid of fertile (FER), Oligo-Astheno-Terato spermia (OAT), and non-obstructive azoospermia (NOA) men. **a** Absolute cell count of CD45<sup>+</sup> cells and pie charts showing the overall leukocyte subset distribution in FER ( $n = 28$ ), OAT ( $n = 35$ ), and NOA ( $n = 8$ ) men; numbers in pie charts indicate the mean, \* $P \leq 0.05$  and \*\* $P \leq 0.01$  vs FER. Lower panels show the distribution of each leukocyte population in the different groups; each dot represents a single donor, scatter plots indicate mean  $\pm$  SEM; Kruskal-Wallis test in association with Dunn's multiple comparison test was used to determine the statistical significance of the data, statistically significant  $P$  values are reported. **b** The proportion of DC-10 (CD11c<sup>+</sup>CD14<sup>+</sup>CD16<sup>+</sup>CD141<sup>+</sup>CD163<sup>+</sup>), cDC1 (CD14<sup>+</sup>CD11c<sup>+</sup>CD141<sup>+</sup>), and cDC2 (CD11c<sup>+</sup>CD1c<sup>+</sup>) in the sperm fluid of FER ( $n = 10$ ), OAT ( $n = 25$ ), and iNOA ( $n = 8$ ) men; the percentage of DC-10 expressing HLA-G and

CD83, and the ratio between the percentage of cDC1 and DC-10 and of cDC2 and DC-10 calculated for each donor are shown. Each dot represents a single donor; scatter plots indicate mean  $\pm$  SEM; the Kruskal-Wallis test, in association with Dunn's multiple comparison test, was used to determine the statistical significance of the data, and statistically significant  $P$  values are reported. **c** The presence and concentration of cytokines and chemokines were evaluated using multi-beads array in sperm plasma of fertile men without (nFER,  $n = 8$ ) or with one/two spermogram alterations (aFER,  $n = 17$ ), OAT ( $n = 32$ ), and NOA ( $n = 7$ ) men. All the analytes tested were divided into different heatmaps according to their concentration (pg/ml); in each heatmap, cytokines/chemokines are ordered based on their abundance. Heat map color corresponds to the real concentration values being the spectrum of blue to green to yellow corresponding to increasing gradient of chemokine/cytokine concentrations. Values above the standard range are reported in orange. Source data are provided as a Source Data file.

semen parameters (nFER) (Figs. 1c and Supplementary Fig. 3). The levels of several pro-inflammatory cytokines, including IL-1 $\beta$ , IL-2, IL-12, IFN $\gamma$ , IL-6, and TNF $\alpha$ , and of almost all pro-inflammatory chemokines analyzed (e.g., MIP-1 $\alpha$ , Eotaxin, Rantes, MIP1 $\beta$ , MCP-1, and IP-10) are higher in the semen of OAT patients compared to nFER men (Fig. 1c and Supplementary Fig. 3). In line with previous reports<sup>28,30</sup>, seminal profile of NOA patients is comparable to that of nFER men, except for some anti-inflammatory (IL-4, IL-13, IL-10, IL-5, IL-1RA) and pro-inflammatory (Eotaxin, TNF $\alpha$ , IL-15, and IP-10) analytes (Fig. 1c and Supplementary Fig. 3). Notably, aFER men display a frequency of neutrophils and CD14<sup>+</sup> cells comparable to that observed in OAT and NOA patients, which in turn is higher than that of nFER men. Conversely, no differences in the proportion of eosinophils, CD3, NK, and NKT cells are observed among groups (Supplementary Fig. 4a). Moreover, a higher proportion of pro-inflammatory cDC1 and cDC2 is observed in OAT and NOA patients as compared with both nFER and aFER men, whilst the frequency of DC-10 is comparable among groups. These data confirm that the semen of infertile men is characterized by a high proportion of pro-inflammatory DC (Supplementary Fig. 4b).

Overall, these data indicate that a pro-inflammatory milieu featured by neutrophils, inflammatory DC, and pro-inflammatory cytokine and chemokines characterizes the semen of OAT and NOA patients. The nature of the semen pro-inflammatory milieu is associated with the presence of aberrant spermatozoa in OAT patients, while the altered immune cell profile of NOA patients might be associated with the cellular senescence previously reported<sup>13</sup>.

### Increased neutrophil and reduced T cell frequency characterize the peripheral blood of infertile patients

An in-depth characterization of the myeloid and lymphoid cell composition in the peripheral blood of infertile and fertile men has been carried out. As reported for the semen, we detect a higher frequency of neutrophils in OAT and NOA patients compared to FER men, reaching a significant difference in OAT patients (Figs. 2a and Supplementary Fig. 5a). Conversely, the frequencies of eosinophils (CD15<sup>+</sup>CD16<sup>+</sup>) and monocytes (CD14<sup>+</sup>) are comparable among groups (Fig. 2a). The frequency of the tolerogenic DC-10 and cDC2 is comparable among OAT, NOA and FER men, while a significantly higher proportion of inflammatory cDC1 is present in OAT patients compared to FER men, resulting into a cDC1/DC-10 ratio significantly higher in OAT patients vs. FER men (Figs. 2a and Supplementary Fig. 5b). We detect an overall reduction in the frequency of circulating T (CD3<sup>+</sup>, CD3<sup>+</sup>CD4<sup>+</sup> and CD3<sup>+</sup>CD8<sup>+</sup>) and B (CD19<sup>+</sup>) cells in infertile compared to FER men, with significant differences in OAT patients (Fig. 2b). Groups do not differ in the proportion of NK, NKT, and regulatory T (Tr1 and FOXP3<sup>+</sup> Treg) cells (Figs. 2b, c, and Supplementary Fig. 5c).

In line with the results obtained in the semen (Fig. 1c), the levels of some pro-inflammatory mediators (e.g., MCP-1, TNF $\alpha$ , Eotaxin, and MIP-1 $\beta$ ) result higher in the plasma of men with OAT, NOA, and aFER compared to nFER men (Fig. 2d and Supplementary Fig. 6).

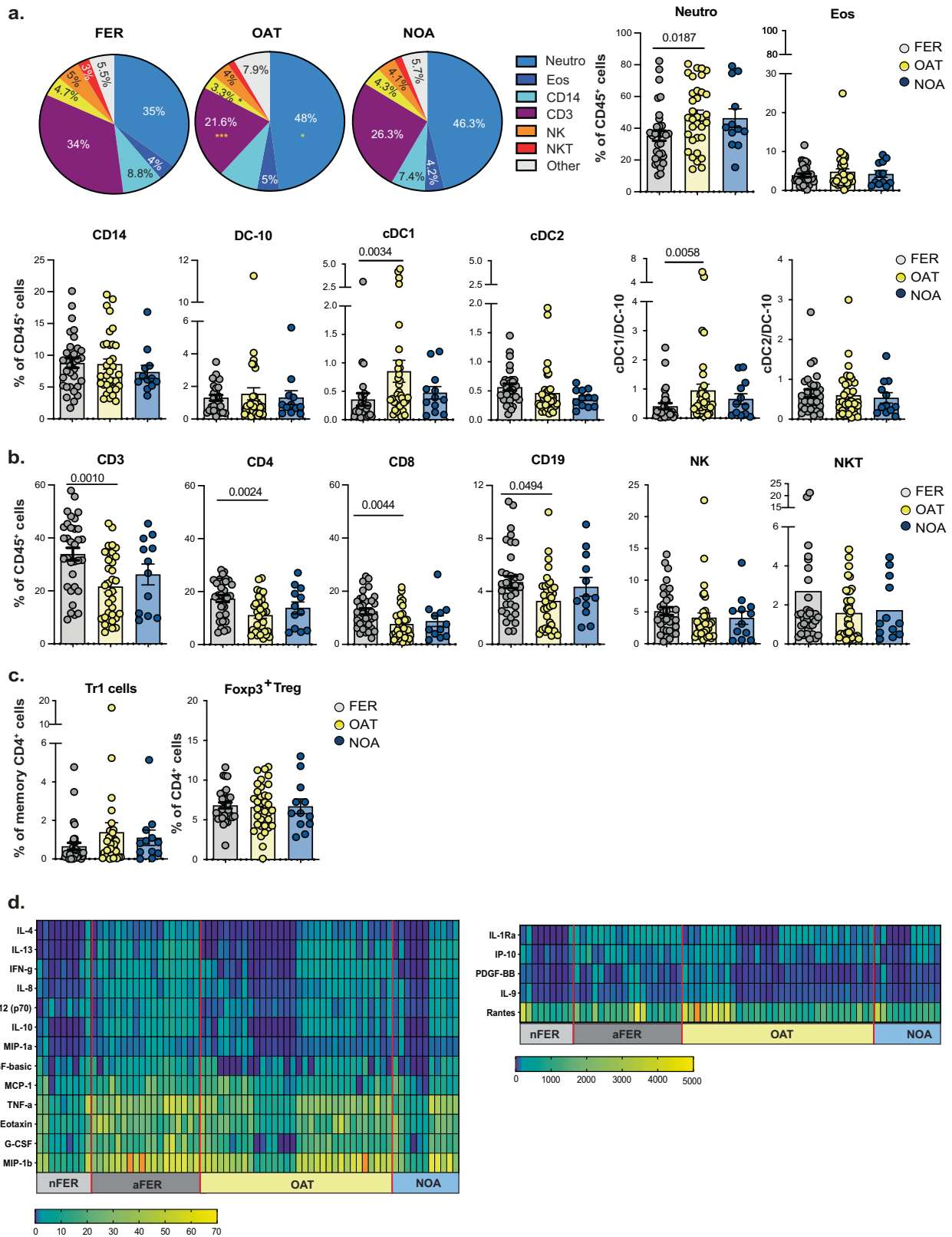
Overall, these analyzes indicate that the peripheral blood of infertile (OAT and NOA) patients is characterized by a higher proportion of neutrophils associated with a reduced frequency of T and B cells, which results in a statistical difference in OAT patients.

### T cells from infertile men exhibit a pro-inflammatory signature

No differences in the proportion of CD4<sup>+</sup> T cells expressing the activation markers HLA-DR, CD25, and LAG-3 in infertile and FER men are identified (Figs. 3a and Supplementary Fig. 7). Conversely, we detect a significantly higher percentage of CD8<sup>+</sup>CD25<sup>+</sup> T cells in OAT and NOA patients compared to FER men, and of CD8<sup>+</sup>LAG-3<sup>+</sup> T cells in OAT patients compared to FER men (Fig. 3a). Interestingly, the percentage of CD4<sup>+</sup> and CD8<sup>+</sup> T cells expressing the inhibitory markers PD-1 and TIM-3 is significantly higher in infertile than those in FER men, and the expression of transcription factors associated with T cell exhaustion (Eomes and T-bet) is higher in CD4<sup>+</sup> T cells from infertile than FER men (Fig. 3a).

Functional characterization of T cells reveals limited differences between infertile and fertile men. Compared to controls, T cells from infertile patients show slightly less proliferative capacity in response to low doses of anti-CD3 mAbs and to PHA (Fig. 3b and Supplementary Fig. 8a); T cells from OAT patients release higher levels of IFN $\gamma$  upon anti-CD3 stimulation compared to T cells from FER men, while the amounts of IL-10 and GM-CSF are comparable (Fig. 3b); PHA-activated T cells from infertile patients show a tendency towards reduced production of GM-CSF, while IFN $\gamma$  and IL-10 production is comparable to T cells from FER men (Fig. 3b). Intracellular flow cytometric analysis shows comparable frequencies of IFN $\gamma$ <sup>+</sup>, IL-4<sup>+</sup>, IL-10<sup>+</sup>, IL-17<sup>+</sup>, and IL-9-producing CD4<sup>+</sup> and of CD8<sup>+</sup> T cells in infertile and FER men. Conversely, in line with the proliferative capacity, a low proportion of IL-2-producing cells is detected in infertile T cells (Figs. 3c and Fig. 4a and Supplementary Fig. 8b). Despite no difference in the frequencies of Th1 and Th2 cells, a lower proportion of Th17 cells and a higher proportion of Th9 cells are detected in infertile compared to fertile men (Fig. 4b, c). Overall, these analyzes reveal an altered phenotype and function of peripheral blood T cells in infertile compared to age-matched FER men.

To further investigate T cell alterations in infertile patients, we performed droplet-based single-cell RNA sequencing (scRNAseq) of CD3<sup>+</sup> T cells purified from the peripheral blood of OAT ( $n = 4$ ), NOA ( $n = 6$ ), and FER ( $n = 5$ ) men (Supplementary Fig. 9a). After quality control filtering, we obtain transcriptional profiles from 45622 T cells (Supplementary Table 2). According to marker genes cluster-specific expression levels, clusters have been manually annotated (Fig. 5a, Supplementary Fig. 9b, and Supplementary Data 1). By UMAP dimensionality reduction, we identify six cell clusters within the CD4<sup>+</sup> population (two CD4<sup>+</sup>FOXP3<sup>+</sup> Tregs, CD4<sup>+</sup>Tfh, CD4<sup>+</sup>Th2, CD4<sup>+</sup>Th1/Th17), six clusters within the CD8<sup>+</sup> population (two CD8<sup>+</sup> naive, CD8<sup>+</sup>TCM GzK<sup>+</sup>, CD8<sup>+</sup>TE Tox<sup>+</sup>, CD8<sup>+</sup>TE GzK<sup>+</sup>, CD8<sup>+</sup>TEM), and two clusters expressing both CD4 and CD8 (CD4<sup>+</sup>CD8<sup>+</sup> and CD4<sup>+</sup>CD8<sup>+</sup>TEM),



with the naïve compartment (SELL<sup>+</sup>CCR7<sup>+</sup>) representing almost 33% of the cells (Figs. 5a and Supplementary Fig. 9c). In both CD4<sup>+</sup> and CD8<sup>+</sup> T cell naïve compartments, we identify two different clusters: naïve and naïve activated (naïve A), with the latter characterized by an increased expression of genes involved in cell cycling (Figs. 5a and Supplementary Fig. 9c). Moreover, we identify a cluster of mucosal-associated

invariant T cells (MAIT, KLRB1<sup>+</sup>GZMK<sup>+</sup>), two clusters of NK cells (CD16<sup>+</sup>FCER1G<sup>+</sup>), and a cluster of TCR  $\gamma/\delta$  T cells (TRDC<sup>+</sup>TRGC1<sup>+</sup>) (Figs. 5a and Supplementary Fig. 9c). All clusters have been detected in each sample of the 3 analyzed groups (Figs. 5a and Supplementary Fig. 9c). As compared with FER men, we detect an expansion of differentiated T cell clusters in OAT and NOA patients, supporting a more

**Fig. 2 | Systemic pro-inflammatory signature in severe infertile men. a–b** The proportion of the major leukocyte subsets and regulatory T cells was analyzed by multiparametric flow cytometry in peripheral blood of fertile (FER,  $n = 33$ ), Oligo-Asthenozoospermia (OAT,  $n = 34$ ), and non-obstructive azoospermia (NOA,  $n = 12$ ) men. **a** Pie charts showing the overall leukocyte subset distribution in FER, OAT, and NOA men; numbers in pie charts indicate the mean,  $*P \leq 0.05$  and  $***P \leq 0.001$  vs. FER; scatter plot (mean  $\pm$  SEM) showing the proportion of the indicated myeloid cell subsets in FER ( $n = 29$ ), OAT ( $n = 34$ ), and NOA ( $n = 12$ ) men and the ratio between the percentage of cDC1 and DC-10 and between the percentage of cDC2 and DC-10 calculated for each donor is presented; each dot represents a single donor; Kruskal-Wallis test in association with Dunn's multiple comparison test were used to determine the statistical significance of the data, statistically significant  $P$  values are reported. **b** The frequencies of the indicated lymphoid cell subsets, including T regulatory type 1 (Tr1, CD4<sup>+</sup>CD45RA<sup>+</sup>CD49b<sup>+</sup>LAG-3<sup>+</sup>) and FOXP3<sup>+</sup> Treg (CD4<sup>+</sup>CD25<sup>+</sup>CD127<sup>+</sup>FOXP3<sup>+</sup>) cells in the peripheral blood of FER ( $n = 33$ ), OAT ( $n = 31$ ), and NOA ( $n = 12$ ) men are shown; each dot represents a single

donor, scatter plots indicate mean  $\pm$  SEM; Kruskal-Wallis test in association with Dunn's multiple comparison test were used to determine the statistical significance of the data. **c** The frequencies of T regulatory type 1 (Tr1, CD4<sup>+</sup>CD45RA<sup>+</sup>CD49b<sup>+</sup>LAG-3<sup>+</sup>) and FOXP3<sup>+</sup> Treg (CD4<sup>+</sup>CD25<sup>+</sup>CD127<sup>+</sup>FOXP3<sup>+</sup>) cells in the indicated cohort of donors are shown; each dot represents a single donor, scatter plots indicate mean  $\pm$  SEM; Kruskal-Wallis test in association with Dunn's multiple comparison test were used to determine the statistical significance of the data. **d** The presence and concentration of cytokines and chemokines were evaluated using a multi-beads array in plasma from peripheral blood of fertile men without (nFER,  $n = 9$ ) or with one/two spermogram alterations (aFER,  $n = 18$ ), OAT ( $n = 32$ ), and NOA ( $n = 11$ ) men. All the analytes tested were divided into two different heatmaps according to their concentration (pg/ml); in each heatmap, cytokines/chemokines are ordered based on their abundance. Heat map color corresponds to the real concentration values, the spectrum of blue to green to yellow, corresponding to an increasing gradient of chemokine/cytokine concentrations. Values above the standard range are reported in orange. Source data are provided as a Source Data file.

activated environment in infertile men; indeed, the sum of the percentages of CD4<sup>+</sup> Tfh, CD4<sup>+</sup> Th2, CD4<sup>+</sup> Th1/Th17, CD8<sup>+</sup> TCM GzK<sup>+</sup>, CD8<sup>+</sup> TE Tox<sup>+</sup>, CD8<sup>+</sup> TE GzK<sup>+</sup>, CD8<sup>+</sup> TEM, CD4<sup>+</sup>CD8<sup>+</sup> and CD4<sup>+</sup>CD8<sup>+</sup> TEM is 48.59% in OAT, 54.31% in iNOA, and 42.42% in FER men, respectively. In line with data obtained from the immunophenotyping, the frequency of CD4<sup>+</sup> FOXP3<sup>+</sup> Tregs does not differ among OAT, NOA, and FER men (Fig. 5a and Supplementary Table 2).

The intracuster gene set enrichment analysis (GSEA) for hallmark molecular database signatures of differentiated T cell subsets (e.g., excluding the naive compartment, TCR  $\gamma/\delta$ , MAIT, NK, and CD4<sup>+</sup>FOXP3<sup>+</sup> Tregs subsets) revealed that T cells from infertile patients are characterized by the downregulation of ESTROGEN response associated genes, and by molecular signatures related to inflammatory responses (Interferon-gamma response, and allograft-rejection) which results significantly enriched compared to FER men (Fig. 5b and Supplementary Data 2). Notably, T cells from NOA, but not from OAT patients, also exhibit enrichment in interferon-alpha response genes compared to FER men (Fig. 5b). Hence, T cells of OAT and NOA patients share common hallmarks that differ from T cells of FER men. Moreover, T cells of OAT and NOA patients display specific and distinct signatures, such as interferon-alpha response that is upregulated in NOA but not in OAT patients.

We show an increased frequency of CD8<sup>+</sup> T cells expressing single markers associated with T cell activation (e.g., CD25 and LAG-3, Fig. 3a); thus, we calculated the activation score of the differentiated T cell subsets by assessing the expression of a panel of well-known T cell activation-associated genes (GO:0042110). Nearly all T cell subsets in OAT patients display a higher activation score compared to both NOA patients and FER men (Fig. 5c and Supplementary Data 3). NOA patients also show the presence of an increased activation score only in some CD8<sup>+</sup> T cell subsets compared to FER men (Fig. 5c and Supplementary Data 3). Notably, cells with the highest score are distributed mainly in the CD8 effector clusters [e.g., CD4<sup>+</sup>CD8<sup>+</sup> TEM, CD8<sup>+</sup> TE (TOX<sup>+</sup>), CD8<sup>+</sup> TE (GzK<sup>+</sup>), and CD8<sup>+</sup> TEM (Fig. 5c)]. The proportion of T cells with an activation score  $>0.25$  is increased in OAT, but not in NOA patients, compared to FER men (Figs. 5d and Supplementary Table 3). These results indicate an overall higher activation status of T cells in OAT patients than in NOA patients and FER men.

### Signatures of exhaustion and senescence distinguish T cells of OAT and NOA patients

We report an increased frequency of both CD4<sup>+</sup> and CD8<sup>+</sup> T cells expressing single markers associated with T cell exhaustion (e.g., LAG-3, KLRG1, PD-1, TIM-3, Eomes, and T-bet; Fig. 3a), thus to investigate the functional state of memory T cell subsets across the three conditions, we score their exhaustion status by assessing the expression of a panel of exhaustion-associated genes (e.g., TOX, TIGIT, PDCD1, CD244 - 2B4,

HAVCR2 - Tim-3, GzK, KLRG1, LAG-3, ITGB1, NFIL3, ITGA2-CD49b, TNFRSF9-4-1BB, TMPO, and TGFB3). T cells from OAT patients exhibit an overall higher exhaustion score compared to cells from NOA patients and FER men, while T cells from both infertile groups show a higher score than FER control in specific T cell clusters (e.g., CD4<sup>+</sup>CD8<sup>+</sup> TEM, CD8<sup>+</sup> TE TOX<sup>+</sup>, CD8<sup>+</sup> TE GzK<sup>+</sup>, and CD8<sup>+</sup> TEM) (Fig. 6a, and Supplementary Data 3). T cells from OAT patients display the highest percentage of cells with an exhaustion score  $>0.25$  compared to both NOA patients and FER men (Figs. 6b and Supplementary Table 3). The applied unsupervised t-distributed stochastic neighbor embedding (tSNE) analysis performed on flow cytometry data from T cells of OAT, NOA, and FER men validates the scRNAseq results, showing a higher expression of TIM-3, PD-1, and KLRG1 both in CD4<sup>+</sup> and CD8<sup>+</sup> T cells of infertile compared to FER men (Supplementary Fig. 10). In line with data presented in Fig. 3a, this analysis confirms a higher proportion of T cells expressing TIM-3 in OAT and NOA patients compared to FER men. Moreover, we observe an overall higher percentage of CD4<sup>+</sup> and CD8<sup>+</sup> T cells co-expressing TIM-3 and PD-1 in OAT than in NOA and FER men (Supplementary Fig. 10). In addition, TIM-3<sup>+</sup>PD-1<sup>+</sup> T cells in OAT patients express Eomes but not T-bet (Supplementary Fig. 10), thus indicating an exhausted phenotype<sup>31,32</sup>. Accordingly, T cells from OAT patients exhibit the highest expression levels of genes included in the exhaustion score panel, while only PDCD1, GzK, KLRG1, and LAG-3 are expressed at high levels in NOA patients (Fig. 6c). Notably, these latter genes have also been associated with T cell senescence<sup>33,34</sup>. Since one of the distinctive features of senescent cells is the expression of genes associated with SASP<sup>35,36</sup>, we calculated the SASP score by testing the expression of SASP Reactome Gene List in the T cell subsets of the three conditions. T cells from NOA patients show a significantly higher SASP score compared to T cells from OAT patients in all clusters (Figs. 6d, and Supplementary Data 3). The percentage of T cells having a SASP score  $>0.25$  is 17.95%, 12.32%, and 15.34% in NOA, OAT and FER men, respectively (Figs. 6d, and Supplementary Table 3). A prominent signature of exhaustion in T cells emerges from OAT patients, whilst of senescence in NOA patients (Fig. 6e). Moreover, exhausted T cells are located within the effector clusters [e.g., CD8<sup>+</sup> TE (GzK<sup>+</sup>), CD4<sup>+</sup>CD8<sup>+</sup> TEM, CD8<sup>+</sup> TE (TOX<sup>+</sup>), CD8<sup>+</sup> TEM, blue dots, Fig. 6e], while T cells with SASP score  $>0.25$  are distributed in CD4<sup>+</sup> Th clusters (red dots, Fig. 6e). Both cell types are poorly represented in FER men.

These novel findings demonstrate a shift toward exhaustion and senescence in peripheral blood T cells in OAT and NOA patients, respectively.

### Discussion

Our novel findings demonstrate that the semen of infertile patients (i.e., OAT and NOA) is characterized by a pro-inflammatory environment with an increased frequency of neutrophils, monocytes, inflammatory DC, and soluble mediators. Of clinical relevance, this pro-

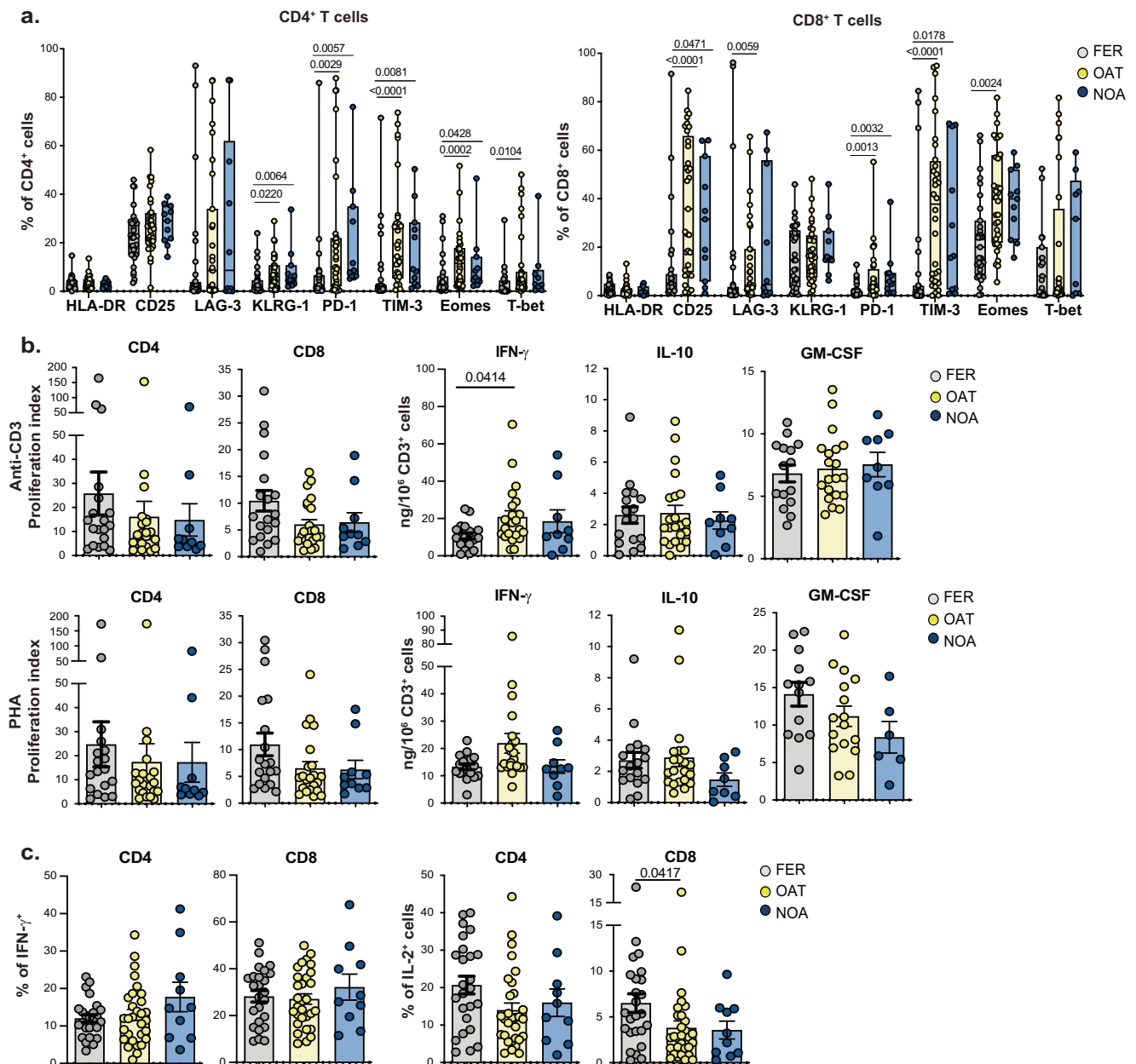


**Fig. 3 | Characterization of peripheral T cells from infertile and fertile men.** **a** The proportion of circulating CD4<sup>+</sup> and CD8<sup>+</sup> T cells expressing the indicated activation and inhibitory markers was analyzed by multiparametric flow cytometry in the peripheral blood of fertile (FER,  $n = 31$ ), Oligo-Astheno-Terato spermia (OAT,  $n = 33$ ), and non-obstructive azoospermia (NOA,  $n = 11$ ) men; bar plots indicate mean  $\pm$  SEM; Kruskal-Wallis test in association with Dunn's multiple comparison test were used to determine the statistical significance of the data; statistically significant  $P$  values are reported. **b–c.** The proliferative capacity and cytokine production of CD3<sup>+</sup> T cells from FER ( $n = 25/n = 18$ ), OAT ( $n = 30/n = 22$ ), and NOA ( $n = 10/n = 10$ ) men in response to different stimuli were tested. **b** PBMC were labeled with proliferation dye and left unstimulated or stimulated with anti-CD3 mAb (upper panels) or phytohemagglutinin (PHA) (lower panels) for four days. The percentage of proliferated cells was evaluated as the percentage of cells that

diluted the dye; proliferation index (PI) represents the ratio between the percentage of CD4<sup>+</sup> and of CD8<sup>+</sup> T cells proliferated in the stimulated condition/percentage of proliferated cells in the unstimulated condition. At the end of the stimulation, culture supernatants were collected and the presence of IFN $\gamma$ , IL-10, and GM-CSF was evaluated by ELISA; each dot represents a single donor, scatter plots indicate mean  $\pm$  SEM; Kruskal-Wallis test in association with Dunn's multiple comparison test were used to determine the statistical significance of the data; statistically significant  $P$  values are reported. **c** PBMC were activated with phorbol 12-myristate 13-acetate/ionomycin (PMA/IONO) for 6 h; the percentages of CD4<sup>+</sup> and CD8<sup>+</sup> T cells producing IFN-g and IL-2 were evaluated by multiparametric flow cytometry; each dot represents a single donor, scatter plots indicate mean  $\pm$  SEM; Kruskal-Wallis test in association with Dunn's multiple comparison test were used to determine the statistical significance of the data. Source data are provided as a Source Data file.

inflammatory signature is also reflected in the peripheral blood, where a high proportion of neutrophils, inflammatory DC, and soluble factors have been found, along with a reduced frequency of T cells. Peripheral T cells from infertile men express genes associated with inflammatory responses. Remarkably, T cells from OAT and NOA patients display a transcriptional profile of exhaustion and senescence, respectively,

thus supporting the presence of a different inflammatory nature between those two infertility conditions. Overall, our study uncovers that: i) the infertile men, while being young and otherwise healthy, display immune changes typically described in healthy elderly men; and ii) OAT and NOA conditions can be discriminated by distinctive T cell features.

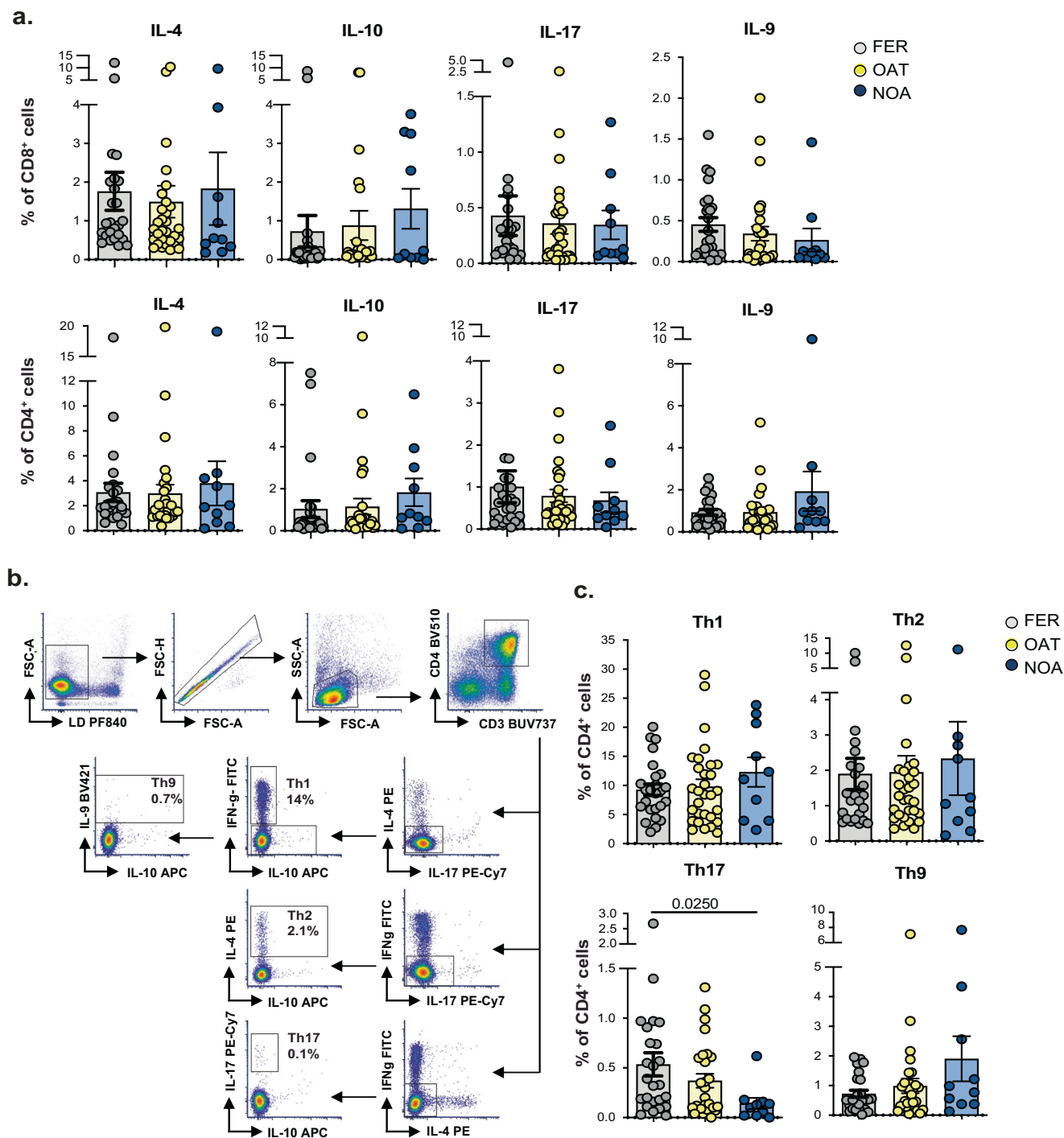
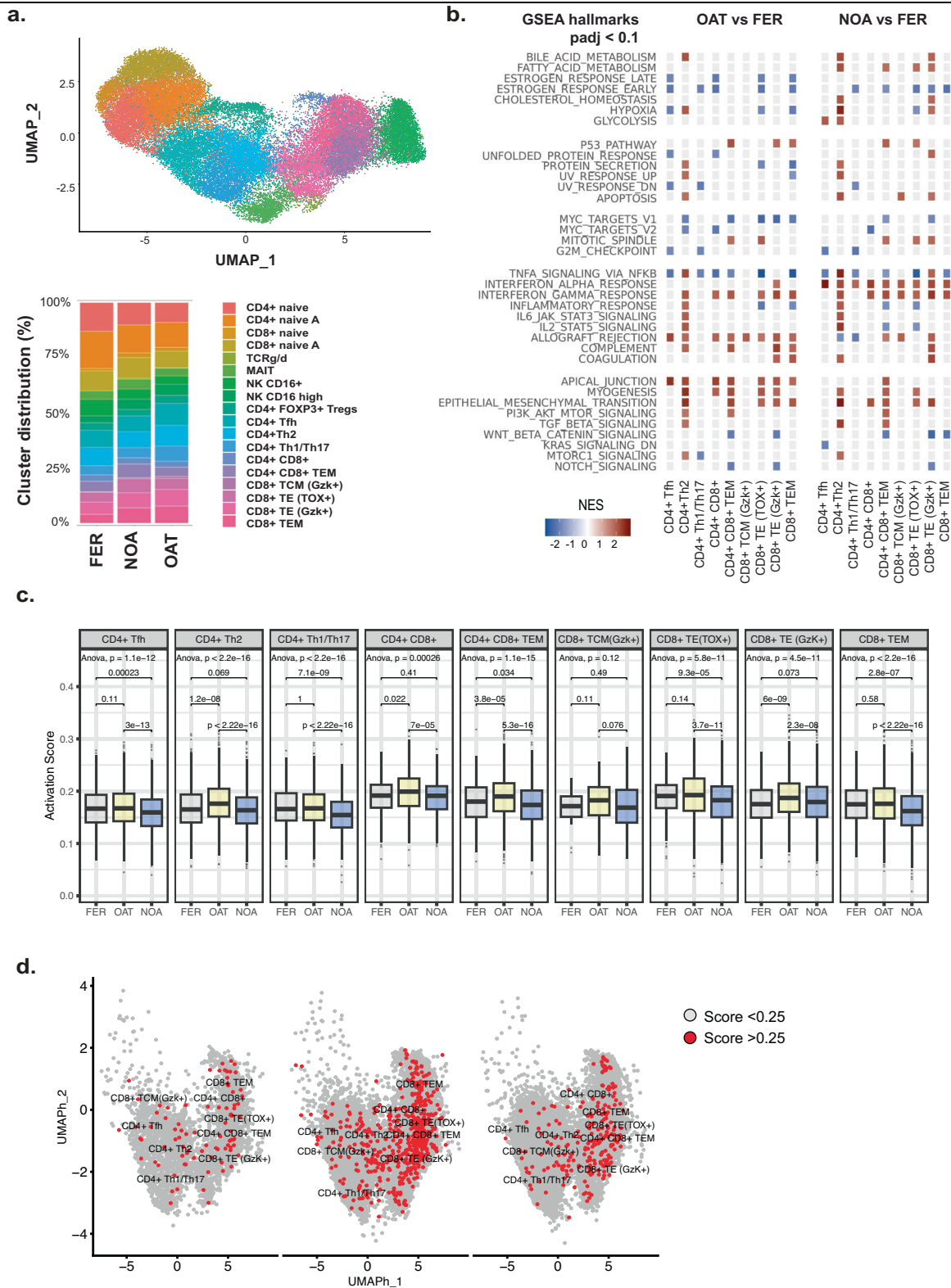


**Fig. 4 | Cytokine production of peripheral blood CD4<sup>+</sup> and CD8<sup>+</sup> T cells from infertile and fertile individuals.** The ability to produce cytokines of CD3<sup>+</sup> T cells in response to phorbol 12-myristate 13-acetate/Ionomycin (PMA/IONO) stimulation was evaluated by multiparametric flow cytometry. PBMC were isolated from fertile (FER, *n* = 25), Oligo-Astheno-Terato spermia (OAT, *n* = 30), and non-obstructive azoospermia (NOA, *n* = 10) men and activated for 6 h. **a** The percentage of CD8<sup>+</sup> and CD4<sup>+</sup> T cells producing the indicated cytokines is shown. Each dot represents a single donor, scatter plots indicate mean ± SEM; Kruskal-Wallis test in association with Dunn's multiple comparison test were used to determine the statistical significance

of the data. **b–c** The frequency of T helper subsets was evaluated in PBMC stimulated with PMA/IONO. **b** Representative gating strategy used to identify the frequencies of Th1 (CD4<sup>+</sup>IL-4-IL-17IFN $\gamma$ ), Th9 (CD4<sup>+</sup>IL-4-IL-17IFN $\gamma$ IL-9<sup>+</sup>), Th2 (CD4<sup>+</sup>IL-17IFN $\gamma$ IL-4<sup>+</sup>), and of Th17 (CD4<sup>+</sup>IL-4IFN $\gamma$ IL-17<sup>+</sup>) cell subsets; numbers indicate the percentage relative to the CD4<sup>+</sup>CD3<sup>+</sup> gate. **c** Frequency of the indicated Th cell subsets among the three groups. Each dot represents a single donor; scatter plots indicate mean ± SEM; the Kruskal-Wallis test, in association with Dunn's multiple comparison tests, was used to determine the statistical significance of the data, and statistically significant *P* values are reported. Source data are provided as a Source Data file.

Leukocytes represent 13% of non-spermatozoa cells in the semen, with granulocytes accounting for 50–60%, macrophages for 20–30%, and T lymphocytes for the remaining 5%<sup>37</sup>. The overall number of seminal leukocytes is higher in infertile than in fertile men<sup>38,39</sup>. Although our analysis does not reveal major differences in

the number of seminal hematopoietic CD45<sup>+</sup> cells between infertile and fertile men, herein, we confirm that granulocytes are the most abundant leukocyte population, with a significantly higher proportion of neutrophils in the semen of OAT and NOA compared to fertile men. These findings are in line with other reports indicating the



presence of oxidative stress and reactive oxygen species in the semen of infertile men<sup>37,40</sup>.

In addition to neutrophils, we identify an enrichment of inflammatory cDC1 (CD11c<sup>+</sup>BDCA-3<sup>+</sup>) and cDC2 (CD11c<sup>+</sup>BDCA-1<sup>+</sup>) cells in the semen of OAT and NOA compared to FER men, with or without sperm alterations. Our results confirm previous observations showing a correlation between a high frequency of myeloid CD11c<sup>+</sup> cells, which

comprises both DC and macrophages<sup>41,42</sup>, and epididymal inflammation in infertile men<sup>43,44</sup>, and provide more detailed information about the myeloid DC composition in the semen. In addition to classical myeloid DC, we also detect DC-10, a subset of tolerogenic DC characterized by the ability to secrete IL-10, which plays a pivotal role in the maintenance of immune tolerance<sup>25,27,45</sup>. DC-10 are present in a comparable proportion and with a similar phenotype in the semen of

**Fig. 5 | Pro-inflammatory transcriptional profile of infertile men peripheral blood T cells.** **a** Uniform manifold approximation and projection (UMAP) embeddings of 45622 single cells from single-cell RNA-sequencing (scRNA-seq) analysis performed on CD3<sup>+</sup> T cells isolated from peripheral blood of fertile (FER,  $n = 5$ ), Oligo-Astheno-Terato spermia (OAT,  $n = 4$ ), and non-obstructive azoospermia (NOA,  $n = 6$ ) men, showing the formation of 18 clusters with the respective labels indicated in the color legend. Each dot corresponds to a single cell, colored by unsupervised clustering (resolution 1.2) (upper panel). Bar plots showing the distribution of each T-cell cluster in the indicated group of men (lower panel). **b** Tile plot of normalized enrichment scores (NES) from gene set enrichment analysis (GSEA) of hallmark terms on differentially expressed genes (DEG) between OAT or NOA and FER men within the indicated clusters; hallmarks (rows) are grouped by semantic similarity; columns represent single-cluster comparisons between the

specified conditions; non-significant enrichment results are plotted in light gray [Benjamini–Hochberg adjusted  $P$  value (padj)  $> 0.1$ ]. **c–d** Transcriptomic analysis of the activation status of the differentiated/effector T cell clusters. **c** Box plots of the activation score across different clusters and conditions; horizontal lines represent median values, with whiskers extending to the farthest data point within a maximum of 1.5X interquartile range; one-way ANOVA for the comparison of the groups and two-sided T test for the pairwise comparisons were applied;  $P$  values from all the comparisons are reported. **d** UMAP representation of cells tested for the activation score in FER ( $n = 3226$  cells), OAT ( $n = 9905$  cells), and NOA ( $n = 9541$  cells) condition; cells are colored according to the expression of the activation score: gray for a score  $< 0.25$ , red for a score  $> 0.25$ ; percentages of cells with a score  $> 0.25$  are indicated for each condition ( $n = 83$ ,  $n = 514$ , and  $n = 217$  cells for FER, OAT, and NOA, respectively). Source data are provided in the Source Data file.

infertile and fertile men, indicating that the myeloid tolerogenic compartment is not impaired in infertile men. Therefore, despite their presence, the high cDC/DC-10 ratio found in the semen of infertile men suggests that the modulatory function of DC-10 might be limited by the increased proportion of inflammatory DC. Notably, we detect increased levels of pro-inflammatory mediators in the semen of OAT but not in NOA patients. High levels of IL-1 $\beta$ , IL-6, and TNF $\alpha$  have been previously associated with high proportions of granulocytes<sup>29</sup> and low-quality spermatozoa<sup>46</sup>. Accordingly, we also detect a high content of seminal pro-inflammatory cytokines in fertile men with sperm abnormalities (aFER). The findings observed in OAT patients and aFER men suggest that the presence of low-quality and viable spermatozoa might activate immune cells to secrete pro-inflammatory mediators, thus leading to the recruitment of neutrophils, monocytes, and DC. While this process is chronic in OAT patients due to their inability to generate healthy spermatozoa, it is transient in fertile men due to the physiological renewal of spermatozoa occurring approximately every two months. The higher proportions of neutrophils and inflammatory DC observed in NOA patients might be likely related to somatic cell senescence in the testis of NOA patients, as has been previously reported<sup>13</sup>.

Markers of chronic inflammation found in the peripheral blood of NOA patients have been associated with early aging of somatic testicular cells<sup>13</sup>. Our findings confirm the presence of a systemic pro-inflammatory signature in the peripheral blood of NOA patients, and we identify a similar condition in OAT patients. In comparison with fertile men, a higher frequency of circulating neutrophils and cDC1 is found in OAT patients and, to a lesser extent, in NOA patients. Moreover, we detect high levels of circulating MCP-1, TNF $\alpha$ , Eotaxin, and MIP-1 $\beta$  associated with myeloid cell activation and/or recruitment in infertile men. Therefore, a systemic pro-inflammatory environment characterizes infertile men. A recent study has shown that systemic blood oxidative stress reflects semen oxidative status in NOA patients<sup>47</sup>; moreover, elevated plasma levels of pro-inflammatory cytokines have been associated with blood-testis barrier dynamics and permeability<sup>48</sup>, sustaining a cross-talk between testis and systemic inflammation in infertile men.

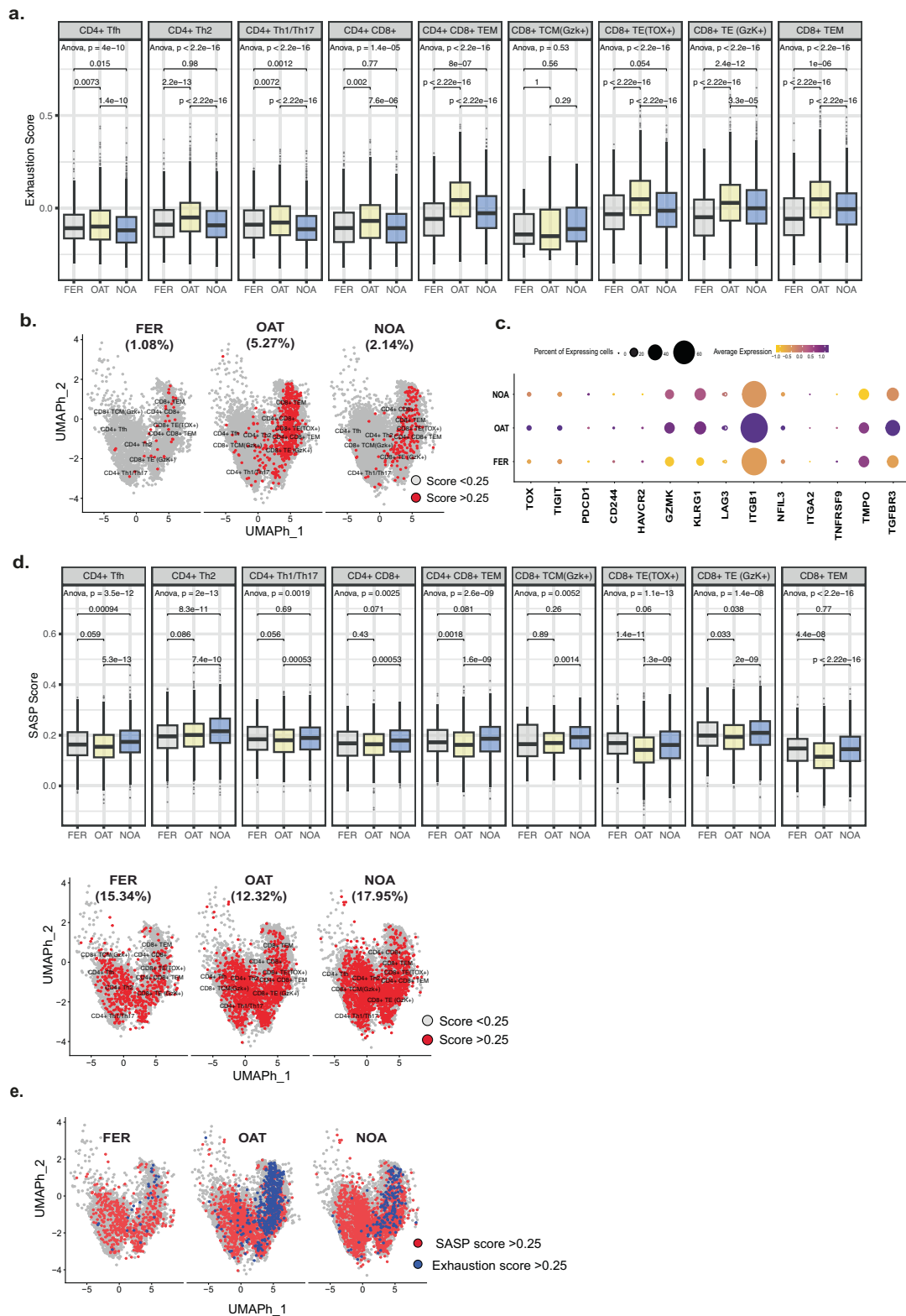
The skew toward the myeloid compartment observed in the peripheral blood of infertile men is associated with an overall reduction in the proportion of CD3<sup>+</sup> T cells. These changes in the peripheral blood cell composition - known as immune senescence - are naturally associated with aging<sup>49,50</sup>. The most prominent decline in lymphocytes and the increase in neutrophils have been reported in healthy elderly men (aged 70–92 years) and have been associated with high levels of TNF $\alpha$  and IL-6<sup>51,52</sup>. Notably, our infertile patients are adult men with a median age of 37 (range 22–54) and 35.5 (range 22–52) years in OAT and NOA patients, respectively. Despite reduced T cells in infertile men display an overall higher rate of differentiated/effector cells, particularly CD8<sup>+</sup> T cells, expressing activation and/or exhaustion markers. Moreover, T cells from OAT and NOA patients display common inflammatory hallmarks and, when activated in vitro, show a reduced

IL-2 production, a feature described in T cells from elderly male men with low-grade inflammation<sup>53</sup>. These features are consistent with the hypothesis of early aging of the immune system in infertile men<sup>50,54</sup> and support the conclusion that infertile men resemble healthy elderly men in terms of immunophenotype.

A growing amount of epidemiologic data has reported a greater proportion of prevalent comorbidities (e.g., those diseases already present before or within 12 months from the diagnosis of infertility)<sup>9,55,56</sup>, and a higher probability of developing NCDs (e.g., if a comorbidity is diagnosed  $\geq 12$  months after the diagnosis of infertility)<sup>57</sup> in infertile men, suggesting that they are overall less healthy than age-comparable fertile individuals. Our findings depict an increased proportion of neutrophils in the peripheral blood of infertile men who were otherwise healthy at the time of recruitment. A high proportion of circulating neutrophils has been described in several diseases, including cancers<sup>58</sup>, and has been reported to be associated with chronic inflammatory diseases, including type 2 diabetes<sup>59</sup> and cardiovascular disease (e.g., atherosclerosis)<sup>60</sup>. The transcriptomic analysis unravels a transcriptional profile of exhaustion for T cells in OAT patients and of senescence for T cells in NOA patients. Exhausted and/or senescent T cells are involved in the pathogenesis of certain age-related diseases (e.g., cardiovascular, metabolic, neurodegenerative, and neoplastic disorders)<sup>20,61</sup>. Of clinical importance, some of these diseases are developed as comorbidities at an earlier age than expected in a significant proportion of severe infertile men<sup>7,8</sup>. Therefore, the early aging of the immune system and divergent T cell differentiation in infertile men described here likely predispose these men to the early development of NDCs.

The study is not devoid of limitations. The relatively small cohort of white-European men may restrict the generalizability of the results and envisages the need to enlarge the study cohorts by including other ethnicities and different infertility conditions (e.g., proven obstructive azoospermia, OAT patients with different etiological factors). Since the semen is a mixture containing sperm and fluids derived from the prostate and the other male accessory glands, the presented analysis does not eventually allow to specifically define the origin of the observed inflammatory status.

Overall, these findings detail an association between severe male infertility and both a local and systemic pro-inflammatory immune status. Likewise, they depict that T cell exhaustion and senescence discriminate between OAT and NOA conditions. The discovery of an abnormal immunophenotype in young age and otherwise clinically healthy infertile men could better explain the pathologic link behind the number of prevalent and incident comorbid conditions previously reported in male infertile individuals. More broad correlation analysis of the immunological status in the semen and at systemic levels, described in this study, in association with clinical parameters, genomic and transcriptomic data, and other important characteristics such as the microbiome status, will define specific signatures to better identify patients at higher risk of earlier developing comorbidities and will be instrumental in developing personalized secondary preventive strategies.



**Methods**

**Human participants**

Infertile men were enrolled at the outpatient clinic of the Division of Experimental Oncology at IRCCS Ospedale San Raffaele, Milan, Italy, and the “Andrology and Reproductive Health Office” at the IRCCS Fondazione Ca’ Granda Ospedale Maggiore Policlinico, Milan, Italy. To

limit potential biases associated with causal heterogeneity of male factor infertility (MFI), only infertile men matching the following inclusion criteria were enrolled in the study: age 18–50 years; non-Finnish, white-European men; belonging to primary infertile couples, with pure MFI. According to the World Health Organization (WHO) criteria, infertility was defined as not conceiving a pregnancy after at

**Fig. 6 | Signatures of exhaustion and senescence distinguish T cells from OAT and NOA men.** Transcriptomic analysis of the exhaustion status of the more differentiated clusters of CD3<sup>+</sup> T cells isolated from peripheral blood of fertile (FER,  $n = 5$ ), Oligo-Asthenoterato spermia (OAT,  $n = 4$ ), and non-obstructive azoospermia (NOA,  $n = 6$ ) men. **a** Box plots of the exhaustion score across different clusters and conditions; horizontal lines represent median values, with whiskers extending to the farthest data point within a maximum of 1.5X interquartile range; one-way ANOVA for the comparison of the groups and two-sided T test for the pairwise comparisons were applied;  $P$  values from all the comparisons are reported. **b** UMAP density plots of cells tested for the exhaustion score in FER ( $n = 3226$  cells), OAT ( $n = 9905$  cells), and NOA ( $n = 9541$  cells) condition; cells are colored according to the expression of the exhaustion score: gray for a score  $< 0.25$ , red for a score  $> 0.25$ ; percentages of cells with a score  $> 0.25$  are indicated for each condition ( $n = 35$ ,  $n = 522$ , and  $n = 205$  cells for FER, OAT, and NOA, respectively). **c** Dot plot showing the expression of genes used to evaluate the exhaustion score across the three conditions; dot size indicates the percentage of cells expressing the queried

gene (columns), color scale represents relative gene expression within each condition (rows). **d** Box plots of the Senescence-Associated Secretory Phenotype (SASP) score across different clusters and conditions; horizontal lines represent median values, with whiskers extending to the farthest data point within a maximum of 1.5X interquartile range; one-way ANOVA for the comparison of the groups and two-sided T test for the pairwise comparisons were applied;  $P$  values from all the comparisons are reported (upper panel). UMAP density plots of cells tested for the SASP score in FER ( $n = 3226$  cells), OAT ( $n = 9905$  cells), and NOA ( $n = 9541$  cells) condition (lower panel); cells are colored according to the expression of the exhaustion score: gray for a score  $< 0.25$ , red for a score  $> 0.25$ ; percentages of cells with a score  $> 0.25$  are indicated for each condition ( $n = 495$ ,  $n = 1221$ , and  $n = 1712$  cells for FER, OAT, and NOA, respectively). **e** UMAP representation of cells tested for the exhaustion and SASP score in FER, OAT, and NOA conditions; blue dots indicated cells with an exhaustion score  $> 0.25$ , and red dots indicated cells with an SASP score  $> 0.25$ . Source data are provided in the Source Data file.

least 12 months of unprotected intercourse regardless of whether a pregnancy ultimately occurs (World Health Organization laboratory manual for the examination and processing of human semen, Sixth edition published on July 2021 (Available at: <https://www.who.int/publications/i/item/9789240030787>). Primary infertility was defined as when a couple was never able to conceive. Age-matched fertile men were recruited via their partners who had been new and expectant mothers in the department of Obstetrics and Gynecology at both recruiting centers and underwent the same comprehensive assessment of the infertile counterpart. All participants were homogeneously assessed by the same expert academic urologist, with a thorough medical history and a complete physical examination (including breast, abdomen, and external genitalia). The Charlson Comorbidity Index (CCI) was used to score health-significant comorbidities, coded using the International Classification of Diseases, 9<sup>th</sup> revision<sup>62</sup>. Both fertile and infertile men with a known history of hematologic disease that could alter their immune profile over the last 6 months were excluded from the study. Oligo-Asthenoterato spermia (OAT) patients included in the study were selected based on two consecutive semen analyzes, and the disease was post-testicular. Non-obstructive azoospermia (NOA) was defined as the complete absence of spermatozoa in the semen in two consecutive semen analyzes<sup>63</sup>.

Venous blood samples were drawn from each patient between 7–11 am after an overnight fast. Chromosomal analysis and genetic testing were performed in every infertile man (karyotype analysis and tests for Y-chromosome microdeletions and cystic fibrosis mutations)<sup>3,64</sup>. According to the WHO laboratory manual for the examination and processing of human semen, 6<sup>th</sup> edition, published in July 2021 (Available at: <https://www.who.int/publications/i/item/9789240030787>)<sup>63,65</sup>, OAT was defined when all anomalies occurred simultaneously, thus including oligozoospermia defined as  $< 15$  million spermatozoa per mL; asthenozoospermia as  $< 32\%$  progressive motility; and teratozoospermia  $< 4\%$  of typical forms. Semen analysis was performed for both fertile and infertile men at the same laboratory, and the latter underwent at least two consecutive semen analyzes<sup>63</sup>. The semen, clinical, and hormonal parameters of enrolled participants are reported in Table 1. Peripheral blood (PB) and semen (SF) samples were collected upon written informed consent in accordance with the Helsinki Declaration and with local ethical committee approvals (Protocols: Creazione di una biobanca di campioni biologici da uomini fertili, CE: 46/INT/2016; Nuovo approccio di “system medicine” per lo sviluppo di strategie di prevenzione primaria delle comorbidità negli uomini infertili, CE 200/INT/2020; protocollo URBANN: 58/INT/2010). All samples have been collected between December 2019 and June 2022.

### Hormonal profile

After an overnight fast, venous blood samples were drawn from each patient (7–11 AM). Follicle-stimulating hormone (FSH; a range of

linearity = 0.3–200 mUI/ml), luteinizing hormone (LH; a range of linearity = 0.3–200 mUI/ml), thyroid-stimulating hormone (TSH; a range of linearity = 0.005–100  $\mu$ UI/ml), and 17 $\beta$ -estradiol (E2; a range of linearity = 5–3000 pg/ml) were measured using a heterogeneous competitive magnetic separation assay (Bayer Immuno 1 System; Bayer Corporation). An enzyme-linked immunosorbent assay was used to measure Inhibin B (Inhibin B Gen II ELISA, Beckman Coulter; a range of linearity = 2.6–1000 pg/ml) and AMH (AMH Gen II ELISA; Beckman Coulter; a range of linearity = 0.01–23 ng/ml). Electrochemiluminescence immunoassay was used for measuring total T levels (tT, Elecsys Testosterone II, Roche; a range of linearity = 0.025–15 ng/ml) and Prolactin (Elecsys Prolactin II, Roche; a range of linearity = 0.1–470 ng/ml). Sex hormone-binding globulin (SHBG) levels were measured via a solid-phase chemiluminescent immunometric assay on the Immulite 2000 (Medical Systems SpA; a range of linearity = 0.02–180 nmol/L). The hormonal dosage has been performed at the same laboratory for every participant.

### Semen analysis

None of the patients had a recent history (e.g., over the last 6 months) or were under medication to improve semen parameters at the time of first assessment. All analyses were performed at the IVF Center, Obstetrics and Gynecology Unit, IRCCS Ospedale San Raffaele, Milan, Italy. Semen samples were collected by masturbation, and semen volume, sperm concentration, and sperm morphology were evaluated within 2 h according to the WHO criteria<sup>63</sup>. The improved Neubauer hemocytometer chamber (100- $\mu$ m-deep; Brand Blaubrand Neubauer Improved Counting Chambers, Fisher Scientific, Loughborough, UK) was used for the calculation of sperm concentration and total sperm count in the ejaculate. Sperm morphology was assessed through the following steps: preparation of a smear of semen on a slide, fixing and staining the slide (Testsimplents Prestained Slides; Waldeck GmbH & Co. KG, Germany), examination with brightfield optics at 1000x magnification (Nikon Eclipse E 200; Nikon Instruments Europe B.V., Italy) with oil immersion and assessment of approximately 200 spermatozoa per replicate for the percentage of normal or abnormal forms. Sperm motility was assessed by mixing the sample twice, using a wet preparation of 20- $\mu$ m-deep for each replicate, by examining the slide with phase contrast optics at 200x magnification, and by assessing approximately 200 spermatozoa per replicate for the percentage of different motile Categories.

### Microbiological analyzes

None of the participants had suggestive symptoms for or a recent history (i.e., over the last 12 months) of male accessory gland infections (MAGIs) (i.e., urethritis, prostatitis, orchitis and epididymitis). In line with an internal research protocol, each participant (both infertile and fertile men) underwent semen and urine culture tests in order to

identify potential common urogenital pathogens. Infections by *Mycoplasma*, *Ureaplasma* and *Chlamydia* spp. have been evaluated through a real time PCR platform (NIMBUS, Seegene, South Korea). Similarly, amplification by nested PCR was used to detect human papillomavirus (HPV)-DNA sequences in all semen samples. PCR was performed at the same laboratory for every participant.

### Flow cytometry analysis on whole blood and semen

The frequencies of major leukocyte populations, of DC-10 and of other monocyte/myeloid populations were assessed by multiparameter flow cytometry on EDTA peripheral blood and on semen within 6 h of sampling. In brief, 50  $\mu$ l of antibody (Abs) mix in brilliant stain buffer (BD biosciences, San Jose, CA) were directly added to 150  $\mu$ l of whole blood and incubated for 15 min at room temperature in the dark. The samples were then incubated for additional 13 min at room temperature in the dark with lysis buffer (EDTA 1 mM, KHCO<sub>3</sub> 10 mM, NH<sub>4</sub>Cl 150 mM) to perform red blood cell lysis and washed twice with phosphate-buffered saline (PBS, Sigma, CA, USA). Finally, samples were stained for 10 min at room temperature (RT) with Live/Dead PromoFluor 840 maleimide reactive dyes (Invitrogen, CA, USA) at a concentration of 0.25  $\mu$ g/ $\mu$ l, washed and re-suspended in PBS (Sigma, CA, USA) with 2% fetal bovine serum (FBS, Lonza, Italy) and 0.5% paraformaldehyde (PFA, Thermo Fisher Scientific, MA, USA). For all the SF samples, the red blood lysis buffer was not performed. Cells were identified using a multiparametric approach based on the combination of the antibodies listed in Supplementary Table 4.

### Flow cytometry staining for T cells

T-cell subsets were identified by multicolor flow cytometry on PBMC using a multiparametric approach based on the combination of the antibodies. The expression of activation markers (e.g., CD25, HLA-DR, and LAG-3), of costimulatory/inhibitory surface molecules (e.g., PD-1, TIM-3, and KLRG-1), and of transcription factors (e.g., FOXP3, Eomes, and t-BET) were analyzed in parallel. Tr1 cells were identified using the combination of CD3, CD4, CD45RA, CD49b, and LAG3 markers<sup>66</sup>. PBMC were isolated via density gradient centrifugation over Lymphoprep (Cedarlane, Canada). After centrifugation, PBMC was collected, and platelets were removed by three low-speed centrifugations. Cells were then re-suspended in PBS (Sigma, CA, USA) and counted.  $5 \times 10^5$  PBMC were stained for 10 min at room temperature (RT) with Live/Dead PromoFluor 840 maleimide reactive dyes (Invitrogen, CA, USA) at a concentration of 0.25  $\mu$ g/ $\mu$ l, washed, re-suspended in 50  $\mu$ l of Abs mix in brilliant stain buffer (BD Biosciences, San Jose, CA), and incubated for 15 min at room temperature in the dark. Finally, cells were washed and re-suspended in PBS (Sigma, CA, USA) with 2% FBS (Lonza, Italy). Cell permeabilization for the evaluation of transcription factors was performed using the Foxp3/Transcription Factor Staining Buffer Set (eBioscience, CA, USA) following manufacturers' instructions. All the antibodies and commercial reagents used are listed in Supplementary Table 4 and Supplementary Table 5.

### Intracytoplasmic staining

$2.5 \times 10^5$  PBMC were left unstimulated or stimulated for 6 h with 50 ng/ml of Phorbol-12-myristate-13-acetate (PMA) and 1 mg/ml of Ionomycin (both from Sigma-Aldrich, MO, USA). 10 mg/ml of Brefeldin A (Sigma-Aldrich, MO, USA) were added for the last 5 h of culture to block granules release. Subsequently, the cells were stained with Live/Dead PromoFluor 840 maleimide reactive dyes (Invitrogen, CA, USA), anti-CD3, and anti-CD4, and fixed in PBS (Sigma, CA, USA) with 2% FBS (Lonza, Italy) and 2% paraformaldehyde (PFA, Thermo Fisher Scientific, MA, USA). The intracellular cytokine staining (ICS) was performed permeabilizing the cells with Saponin 0.5% (Sigma-Aldrich, MO, USA) and staining with anti-IFN $\gamma$ , anti-IL-2, anti-IL-4, anti-IL-9, anti-IL-10, and anti-IL-17 Abs (all from Biosciences, NJ, USA) at room temperature in

the dark for 30 min. Cells were washed once with Saponin 0.5%, once with 200  $\mu$ l of PBS-2%FBS, and then re-suspended in PBS (Sigma, CA, USA) with 2% FBS (Lonza, Italy). All the antibodies and the commercial reagents used are listed in Supplementary Table 4 and Supplementary Table 5.

### T cell proliferation and activation status

$3 \times 10^6$  PBMC were stained with 10 mM of Cell Proliferation Dye eFluor<sup>®</sup> 450 (Invitrogen, CA, USA), according to the manufacturer's instructions, and plated at a concentration of  $10^6$  cells/ml in a final volume of 200 ml of completed X-VIVO 15 (Lonza, NC, USA) in 96-flat well culture plates. Cells were activated or not with soluble CD3 monoclonal Ab (MACS<sup>®</sup> GMP CD3 pure, Miltenyi Biotech, Germany) at a final concentration of 0.05 mg/ml or with Phytohemagglutinin (PHA, Merck, Darmstadt, Germany) at a final concentration of 1 mg/ml. After 4 days, supernatants were collected, and cells were harvested, washed with PBS (Sigma, CA, USA), and stained for 10 min with Live/Dead PromoFluor 840 maleimide reactive dyes (Invitrogen, CA, USA). Cells were then washed with PBS 2% FBS and re-suspended in 50 mL of antibody mixture that included the following mAbs: anti-CD3 and anti-CD4. T cells proliferation was evaluated by flow cytometry through Cell Proliferation Dye eFluor<sup>®</sup> 670 dilution (eBioscience, CA, USA). The percentage of proliferated cells was evaluated as the percentage of cells experiencing at least one round of division.

Levels of IL-10, IFN $\gamma$ , and GM-CSF were evaluated in culture supernatants by standard sandwich ELISA, with purified and biotinylated antibody couples (Becton Dickinson, CA, USA). The standard curves were created diluting rhIL-10 (CellGeniX, Germany), rhIFN $\gamma$  (R&D Systems, MN, USA), and rhGM-CSF (Miltenyi Biotech, Germany) in PBS with 2% of bovine serum albumin at the concentration defined by the manufacturer and the limits of detection were: IL-10: 15 pg/mL, IFN $\gamma$ : 30 pg/mL and GM-CSF: 30 pg/mL. The acquisition was performed using Multiskan-go Reader (Thermo Fisher Scientific, MA, USA) and analyzed with SkanIt<sup>™</sup> Software for Microplate Readers (Thermo Fisher Scientific, MA, USA). The amount of IL-10, IFN $\gamma$ , and GM-CSF detected is shown as ng/1M of cells since every analyte has been normalized based on the percentage of CD3<sup>+</sup> T cells detected by flow cytometry for each donor. All the antibodies and the commercial reagents used are listed in Supplementary Table 4 and Supplementary Table 5.

### Detection of cytokines and chemokines

Plasma from EDTA peripheral blood and sperm fluid were obtained after two rounds of centrifugation at room temperature at 400 g for 15 min and at 700 g for 10 min. All the samples were processed within 2 h of collection and stored immediately at  $-80$  °C until use. The presence of cytokines and chemokines in plasma from peripheral blood and sperm fluid was evaluated by Bio-Plex Pro Human Cytokine Screening Panel, 27Plex (Bio-Rad, CA, USA) according to the manufacturer's instructions. The acquisition was performed using Bio-Plex<sup>®</sup> MAGPIX<sup>™</sup> Multiplex Reader (BIO-RAD, CA, USA) and analyzed with Bio-plex manager (BIO-RAD, CA, USA) software. All the commercial reagents used are listed in Supplementary Table 5.

### Flow cytometry sample acquisition and analysis

All the samples were acquired within 12 h of the staining using a FACS Cytoflex LX flow cytometer (Becton Dickinson, Mountain View, CA). To ensure a standardized sample analysis evaluation among samples, flow cytometer was calibrated daily using 8-peak rainbow calibration particles (Spherotech, IL, USA) before sample acquisition. Data were analyzed with FCS express v7 (De Novo Software, CA, USA), and quadrant markers were set according to the relative fluorescence minus one (FMO) staining performed for all the donors analyzed. All the stainings have been performed in the presence of live/dead

reagents and the analyzes have been performed by excluding dead cells and doublets.

### High-dimensional single-cell data preprocessing and analysis by t-distributed stochastic neighbor embedding (tSNE)

14-Parameter Flow Cytometry Standard (FCS) 3.0 files were imported into FCS express v7 (De Novo Software, CA, USA) and left untreated or hyperlog transformed (the same transformation for all files, prior to tSNE analysis). Following transformation, 14-parameter samples were assigned with a unique file identifier code, concatenated, compensated, and analyzed to identify CD3<sup>+</sup>CD4<sup>+</sup> and CD3<sup>+</sup>CD8<sup>+</sup> T cells. To reduce the size of the input dataset, downsampling to  $3 \times 10^4$  cells from a total of approximately  $5 \times 10^5$  CD3<sup>+</sup>CD4<sup>+</sup> cells and to  $3 \times 10^4$  cells from a total of approximately  $4 \times 10^5$  CD3<sup>+</sup>CD8<sup>+</sup> T cells were applied. Markers included in the analysis were: CD45RA, CD62L, TIM-3, PD-1, KLRG-1, T-bet, and Eomes. The following parameters were tuned for both CD3<sup>+</sup>CD4<sup>+</sup> and CD3<sup>+</sup>CD8<sup>+</sup> analysis: approximation algorithm, Barnes-Hut 0.5; iterations, 500; perplexity, 30.

### Preparation of libraries for Single-cell RNA (scRNA) sequencing

CD3<sup>+</sup> T cells were isolated from PBMC obtained by FER ( $n = 5$ ), OAT ( $n = 4$ ), and NOA ( $n = 6$ ) men by magnetic beads negative selection (Miltenyi Biotech, Germany). Single-cell libraries were generated through the Chromium Single-Cell Controller using the Chromium Single Cell 3' Reagent kit v3.1 according to the manufacturers' instructions. (10X Genomics, CA, USA). For each donor, samples were loaded to obtain a target cell recovery of 8000 cells. After generation of nanoliter-scale Gel bead-in-EMulsions (GEMs), GEMs were reverse transcribed in a T100 Thermal Cycler (Bio-Rad, CA, USA) at 53 °C for 45 min, followed by 85 °C for 5 min, and held at 4 °C. Single-cell droplets were broken, and the single-strand cDNA was isolated and cleaned with Cleanup Mix containing Dynabeads™ MyOne™ Silane (Thermo Fisher Scientific, MA, USA). cDNA was amplified using 13 PCR cycles, and then fragmented, end-repaired, A-tailed and adapter ligated, with SPRIselect Reagent Kit (Beckman Colter, CA, USA) cleanup in between steps according to the manufacturers' instructions. scRNAseq library concentration was determined using Qubit dsDNA HS Assay kit (Thermo Fisher Scientific, MA, USA) at Qubit 3.0, and size distribution was assessed using an Agilent D1000 TapeStation system (Agilent, CA, USA). Libraries were sequenced on Illumina Nova-Seq6000 instruments with a paired-end 150-bp (performed by GENE-WIZ, Germany). All the commercial reagents used are listed in Supplementary Table 5.

### Single-cell RNA (scRNA) sequencing data processing

Base call files obtained as a result of the Illumina sequencing were converted into FASTQ files and processed by *Cell Ranger Single-Cell Software Suite* (version 6.1.1, 10X Genomics) using default parameters. Briefly, the demultiplexed samples were aligned against the human GRCh38 reference genome employing *STAR* aligner (v2.7.0 d). Cell barcodes were extracted and UMIs count gene quantification was performed. Filtered expression matrices generated using Cell Ranger count were imported into R and processed with the *Seurat package* (<http://satijalab.org/seurat> v4.0.3). Each sample was pre-processed and cells with mitochondrial RNA percentages higher than 10 and a number of features <1200 or >6000, were filtered out. Seurat objects were merged, and downstream analysis was performed on a single full dataset.

UMI counts were normalized using *NormalizeData* function, multiplied by a 10,000 scale factor and then transformed to a log scale (normalization.method = "LogNormalize", scale.factor = 10,000). After normalization, the top 20% most variable genes were selected for downstream analysis by using the *FindVariableGenes* function. Data were scaled and regressed outsources of unwanted variability (e.g., the absolute count of RNAs in each cell, the percentage of mitochondrial

genes, the difference between the cell cycle phases scores) by using the *ScaleData* function. The first 100 principal components (PCs) from PCA analysis were employed to remove the donor-derived batch effect by running the Harmony data integration approach (*Harmony package* v1.0, using orig.ident as batch variable). After batch correction, dimensionality reduction was performed on the top 55 harmony-corrected PCs. For cell clustering, a K-nearest neighbor (KNN) graph was first constructed based on the Euclidean distance using the *FindNeighbors* function, with the KNN algorithm set to 20. Subsequently, the modularity optimization technique was applied using the Louvain algorithm through the *FindCluster* function, with resolution parameters set to 1.2. Uniform Manifold Approximation and Projection (UMAP) was applied by running the *RunUMAP* function for two-dimensional visualization.

### Differential analysis and cell-type annotation

Marker genes for each cluster were identified using the *FindAllMarkers* Seurat function with the logfc.threshold argument set to 0.25. Only genes expressed in at least 25% of cells in one of the compared clusters were considered (min.pct = 0.25). Genes with  $p$ -values <  $1e10^{-5}$  from the Wilcoxon Rank Sum test were considered as markers for a specific cluster. The *SingleR* package, with the independent reference *Human Primary Cell Atlas* annotation dataset<sup>67</sup> was employed to remove contaminating cells (B cells, hematopoietic stem cells, myeloid cells, and neutrophils) from the full dataset. Additionally, clusters of cells expressing both myeloid (CD14) and T cell markers (CD3E, CD3G, CD3D, and CD8A) were identified as doublets and subsequently excluded. After cleaning steps, the dataset underwent a normalization process, followed by a principal component analysis with 55 PCs. Cluster identification was then performed with a resolution of 1.2, and marker detection was carried out using the previously mentioned parameters. Overall, 45622 cells were retained over 15 samples, resulting in the identification of 18 clusters. Cell types were manually annotated and assigned to each cluster based on the expression of known cell-type markers. Downstream analyzes were conducted on a subset of this full latter dataset (total number of cells = 22672), including only the following clusters: CD4<sup>+</sup> Tfh, CD4<sup>+</sup> Th2, CD4<sup>+</sup> Th1/Th17, CD8<sup>+</sup> TCM Gzk<sup>+</sup>, CD8<sup>+</sup> TE TOX<sup>+</sup>, CD8<sup>+</sup> TE Gzk<sup>+</sup>, CD8<sup>+</sup> TEM, CD4<sup>+</sup>CD8<sup>+</sup> and CD4<sup>+</sup>CD8<sup>+</sup> TEM.

### GSEA enrichment analysis

Intra-cluster comparisons among the FER, NOA, and OAT conditions were conducted using the FindMarkers function, setting test.use = wilcox, a logFC threshold = 0, min.cells.group = 5 and return.thresh parameter equal to 1. Subsequently, the GSEA function of the ClusterProfiler R package (v3.8.1) was applied, using the full marker gene list ranked by decreasing logFC and the hallmarks gene set (h.all.v7.4.symbols.gmt). Gene sets were considered enriched if their adjusted  $p$ -value was < 0.1. A custom tile plot was produced from GSEA of hallmark terms on DEG between OAT vs FER and NOA vs FER conditions within the annotated clusters, by using the ggplot2 R package (v4.1.3).

### Definition of cell state score (activation, exhaustion, and SASP state score)

To assess the activities of functional expression programs in FER, NOA and OAT conditions, the gene signatures scores were computed using the AddModuleScore function with default parameters. Briefly, for T cell activation (GO:0042110), for exhaustion (TOX, TIGIT, PDCD1, CD244 - 2B4, HAVCR2 - Tim-3, GzK, KLRG1, LAG-3, ITGB1, NFIL3, ITGA2 - CD49b, TNFRSF9 - 4-1BB, TMPO, and TGFBR3), for SASP (R-HSA-2559582) signatures were mapped on scRNAseq data. The average expression of each program was computed at the single-cell level and then corrected by subtracting the mean expression value of 100 randomly selected control genes.

For each cell state score, a box plot was generated using the *ggplot2* R package to visualize the distribution of scores across different clusters and conditions. To evaluate the significance of the scores across the experimental conditions (FER, OAT, and NOA), a One-way Analysis of Variance (ANOVA) was conducted using the *anova* function. A *P*-value < 0.05 indicates the presence of significant differences between the conditions and when significance was reached, the Wilcoxon test was performed (*wilcox.test* function) to calculate significance within clusters. The resulting *P*-values were adjusted for multiple testing by applying Bonferroni's correction. All statistical analyses were performed using R package (v.4.1.3).

### Statistical methods

Throughout the manuscript, data are presented as mean ± SEM as indicated in the Figure/Table legends. For each variable, when comparing more than two groups with the aim of performing all pairwise comparisons, the Kruskal-Wallis test was employed, followed by post-hoc analysis through Dunn's tests, and *p*-values were adjusted with Bonferroni's correction. Dunn's multiple comparison test was performed comparing the mean rank of each group with the mean rank of the FER group in Supplementary Figs. 3, Supplementary Fig. 4, and Supplementary Fig. 6. For Supplementary Table 1 two-sided Mann-Whitney test was used for testing the difference between groups. In all analyses, the significant level was set at 0.05.

Statistical analyses were performed using GraphPad Prism 9.0 version 9.3.1 (GraphPad Software, Inc., CA, USA; <https://www.graphpad.com>). Statistical analyses of scRNA Seq data were performed using R version 4.1.3. (<http://www.R-project.org>).

Figures were created using GraphPad Prism 9.0 version 9.3.1 (GraphPad Software, Inc., CA, USA; <https://www.graphpad.com>).

### Reporting summary

Further information on research design is available in the Nature Portfolio Reporting Summary linked to this article.

### Data availability

All data are included in the Supplementary Information or available from the Authors, as are unique reagents used in the Article. The raw numbers for charts and graphs are available both in the Source Data file and have been deposited at the San Raffaele Open Research Data Repository at the following <https://doi.org/10.17632/xvvggt53m4w.1>. Single-cell RNA sequencing data have been deposited at GEO at the following link: <https://www.ncbi.nlm.nih.gov/geo/query/acc.cgi?acc=GSE253279>. Source data are provided with this paper.

### Code availability

Custom codes used in this article has been deposited to Zenodo (<https://doi.org/10.5281/zenodo.14628680>) [<https://zenodo.org/records/14628680>].

### References

1. Boivin, J., Bunting, L., Collins, J. A. & Nygren, K. G. International estimates of infertility prevalence and treatment-seeking: potential need and demand for infertility medical care. *Hum. Reprod.* **22**, 1506–1512 (2007).
2. Ventimiglia, E. et al. Extensive assessment of underlying etiological factors in primary infertile men reduces the proportion of men with idiopathic infertility. *Front Endocrinol. (Lausanne)* **12**, 801125 (2021).
3. Minhas, S. et al. European association of urology guidelines on male sexual and reproductive health: 2021 update on male infertility. *Eur. Urol.* **80**, 603–620 (2021).
4. Schlegel, P. N. et al. Diagnosis and treatment of infertility in men: AUA/ASRM guideline part I. *Fertil. Steril.* **115**, 54–61 (2021).
5. Eisenberg, M. L. et al. Male infertility. *Nat. Rev. Dis. Prim.* **9**, 49 (2023).
6. Salonia, A. et al. Are infertile men less healthy than fertile men? Results of a prospective case-control survey. *Eur. Urol.* **56**, 1025–1031 (2009).
7. Fallara, G., et al. A systematic review and meta-analysis on the impact of infertility on men's general health. *Eur Urol Focus* **10**, 98–106 (2023).
8. Boeri, L. et al. Risk of health status worsening in primary infertile men: a prospective 10-year follow-up study. *Andrology* **10**, 128–136 (2022).
9. Del Giudice, F. et al. The association between mortality and male infertility: systematic review and meta-analysis. *Urology* **154**, 148–157 (2021).
10. Houston, B. J. et al. A systematic review of the validated monogenic causes of human male infertility: 2020 update and a discussion of emerging gene-disease relationships. *Hum. Reprod. Update* **28**, 15–29 (2021).
11. Alfano, M. et al. Impaired testicular signaling of vitamin A and vitamin K contributes to the aberrant composition of the extracellular matrix in idiopathic germ cell aplasia. *Fertil. Steril.* **111**, 687–698 (2019).
12. Alfano, M. et al. Testicular microbiome in azoospermic men—first evidence of the impact of an altered microenvironment. *Hum. Reprod.* **33**, 1212–1217 (2018).
13. Alfano, M. et al. Aging, inflammation and DNA damage in the somatic testicular niche with idiopathic germ cell aplasia. *Nat. Commun.* **12**, 5205 (2021).
14. Steinbach, E. C. & Plevy, S. E. The role of macrophages and dendritic cells in the initiation of inflammation in IBD. *Inflamm. Bowel Dis.* **20**, 166–175 (2014).
15. Coussens, L. M. & Werb, Z. Inflammation and cancer. *Nature* **420**, 860–867 (2002).
16. Kany, S., Vollrath, J. T. & Relja, B. Cytokines in inflammatory disease. *Int. J. Mol. Sci.* **20**, 6008 (2019).
17. Chaudhry, A. & Rudensky, A. Y. Control of inflammation by integration of environmental cues by regulatory T cells. *J. Clin. Invest* **123**, 939–944 (2013).
18. Amodio, G. et al. Role of myeloid regulatory cells (MRCs) in maintaining tissue homeostasis and promoting tolerance in autoimmunity, inflammatory disease and transplantation. *Cancer Immunol. Immunother.* **68**, 661–672 (2019).
19. Zhao, H. et al. Inflammation and tumor progression: signaling pathways and targeted intervention. *Signal Transduct. Target Ther.* **6**, 263 (2021).
20. Akbar, A. N. & Henson, S. M. Are senescence and exhaustion intertwined or unrelated processes that compromise immunity? *Nat. Rev. Immunol.* **11**, 289–295 (2011).
21. Wherry, E. J. T cell exhaustion. *Nat. Immunol.* **12**, 492–499 (2011).
22. Paramos-de-Carvalho, D., Jacinto, A. & Saude, L. The right time for senescence. *Elife* **10**, e72449 (2021).
23. Herranz, N. & Gil, J. Mechanisms and functions of cellular senescence. *J. Clin. Invest* **128**, 1238–1246 (2018).
24. Khodamoradi, K. et al. Laboratory and clinical management of leukocytospermia and hematospermia: a review. *Ther. Adv. Reprod. Health* **14**, 2633494120922511 (2020).
25. Gregori, S. et al. Differentiation of type 1 T regulatory cells (Tr1) by tolerogenic DC-10 requires the IL-10-dependent ILT4/HLA-G pathway. *Blood* **116**, 935–944 (2010).
26. Amodio, G. et al. Hla-g expression levels influence the tolerogenic activity of human DC-10. *Haematologica* **100**, 548–557 (2015).
27. Amodio, G. et al. Altered Frequency and Phenotype of HLA-G-Expressing DC-10 in Type 1 Diabetes Patients at Onset and in Men at Risk to Develop the Disease. *Front Immunol.* **12**, 750162 (2021).
28. Havrylyuk, A., Chopyak, V., Boyko, Y., Kril, I. & Kurpysz, M. Cytokines in the blood and semen of infertile patients. *Cent. Eur. J. Immunol.* **40**, 337–344 (2015).

29. Politch, J. A., Tucker, L., Bowman, F. P. & Anderson, D. J. Concentrations and significance of cytokines and other immunologic factors in semen of healthy fertile men. *Hum. Reprod.* **22**, 2928–2935 (2007).
30. Maegawa, M. et al. A repertoire of cytokines in human seminal plasma. *J. Reprod. Immunol.* **54**, 33–42 (2002).
31. Henning, A. N., Roychoudhuri, R. & Restifo, N. P. Epigenetic control of CD8(+) T cell differentiation. *Nat. Rev. Immunol.* **18**, 340–356 (2018).
32. Li, J., He, Y., Hao, J., Ni, L. & Dong, C. High Levels of Eomes Promote Exhaustion of Anti-tumor CD8(+) T Cells. *Front Immunol.* **9**, 2981 (2018).
33. Zhang, J., He, T., Xue, L. & Guo, H. Senescent T cells: a potential biomarker and target for cancer therapy. *EBioMedicine* **68**, 103409 (2021).
34. Lee, K. A. et al. Characterization of age-associated exhausted CD8(+) T cells defined by increased expression of Tim-3 and PD-1. *Aging Cell* **15**, 291–300 (2016).
35. Acosta, J. C. et al. A complex secretory program orchestrated by the inflammasome controls paracrine senescence. *Nat. Cell Biol.* **15**, 978–990 (2013).
36. Kuilman, T. et al. Oncogene-induced senescence relayed by an interleukin-dependent inflammatory network. *Cell* **133**, 1019–1031 (2008).
37. Tremellen, K. & Tunc, O. Macrophage activity in semen is significantly correlated with sperm quality in infertile men. *Int J. Androl.* **33**, 823–831 (2010).
38. Smith, D. C., Barratt, C. L. & Williams, M. A. The characterisation of non-sperm cells in the ejaculates of fertile men using transmission electron microscopy. *Andrologia* **21**, 319–333 (1989).
39. Wolff, H. The biologic significance of white blood cells in semen. *Fertil. Steril.* **63**, 1143–1157 (1995).
40. Alahmar, A. T. Role of oxidative stress in male infertility: an updated review. *J. Hum. Reprod. Sci.* **12**, 4–18 (2019).
41. Stanislavov, R. Leukocytes in human seminal fluid. *Akush Ginekol. (Sofia)* **38**, 20–21 (1999).
42. Chen, G. & Zheng, B. Effect of macrophages in semen on sperm quality. *Reprod. Biol. Endocrinol.* **19**, 38 (2021).
43. Duan, Y. G. et al. Dendritic cells in semen of infertile men: association with sperm quality and inflammatory status of the epididymis. *Fertil. Steril.* **101**, 70–77 e73 (2014).
44. Duan, Y. G. et al. Characterisation of dendritic cell subsets in chronically inflamed human epididymis. *Andrologia* **48**, 431–440 (2016).
45. Gregori, S., Amodio, G., Passerini, L. & Santoni de Sio, F. R. Alteration of interleukin-10-producing Type 1 regulatory cells in autoimmune diseases. *Curr. Opin. Hematol.* **29**, 218–224 (2022).
46. Mongioi, L. M. et al. Evaluation of seminal fluid leukocyte subpopulations in patients with varicocele. *Int J. Immunopathol. Pharm.* **34**, 2058738420925719 (2020).
47. Becatti, M. et al. Blood leukocyte ROS production reflects seminal fluid oxidative stress and spermatozoa dysfunction in idiopathic infertile men. *Antioxidants (Basel)* **12**, 479 (2023).
48. Zhang, H. et al. Interleukin-6 disrupts blood-testis barrier through inhibiting protein degradation or activating phosphorylated ERK in Sertoli cells. *Sci. Rep.* **4**, 4260 (2014).
49. Quan, X. Q. et al. Age-related changes in peripheral T-cell subpopulations in elderly individuals: an observational study. *Open Life Sci.* **18**, 20220557 (2023).
50. Kverneland, A. H. et al. Age and gender leucocytes variances and references values generated using the standardized ONE-Study protocol. *Cytom. A* **89**, 543–564 (2016).
51. Valiathan, R., Ashman, M. & Asthana, D. Effects of ageing on the immune system: infants to elderly. *Scand. J. Immunol.* **83**, 255–266 (2016).
52. Bruunsgaard, H., Pedersen, M. & Pedersen, B. K. Aging and proinflammatory cytokines. *Curr. Opin. Hematol.* **8**, 131–136 (2001).
53. Bruunsgaard, H., Skinhoj, P., Pedersen, A. N., Schroll, M. & Pedersen, B. K. Ageing, tumour necrosis factor-alpha (TNF-alpha) and atherosclerosis. *Clin. Exp. Immunol.* **121**, 255–260 (2000).
54. Marquez, E. J. et al. Sexual-dimorphism in human immune system aging. *Nat. Commun.* **11**, 751 (2020).
55. Chen, T., Belladelli, F., Del Giudice, F. & Eisenberg, M. L. Male fertility as a marker for health. *Reprod. Biomed. Online* **44**, 131–144 (2022).
56. Murugappan, G., Li, S., Alvero, R. J., Luke, B. & Eisenberg, M. L. Association between infertility and all-cause mortality: analysis of US claims data. *Am. J. Obstet. Gynecol.* **225**, 57 e51–57 e11 (2021).
57. Burke, N. D. et al. Male infertility and somatic health - insights into lipid damage as a mechanistic link. *Nat. Rev. Urol.* **19**, 727–750 (2022).
58. Schmidt, H. et al. Elevated neutrophil and monocyte counts in peripheral blood are associated with poor survival in patients with metastatic melanoma: a prognostic model. *Br. J. Cancer* **93**, 273–278 (2005).
59. Wiersma, J. J. et al. Diabetes mellitus type 2 is associated with higher levels of myeloperoxidase. *Med Sci. Monit.* **14**, CR406–CR410 (2008).
60. Silvestre-Roig, C., Braster, Q., Ortega-Gomez, A. & Soehnlein, O. Neutrophils as regulators of cardiovascular inflammation. *Nat. Rev. Cardiol.* **17**, 327–340 (2020).
61. Chou, J. P. & Effros, R. B. T cell replicative senescence in human aging. *Curr. Pharm. Des.* **19**, 1680–1698 (2013).
62. Charlson, M. E., Pompei, P., Ales, K. L. & MacKenzie, C. R. A new method of classifying prognostic comorbidity in longitudinal studies: development and validation. *J. Chronic Dis.* **40**, 373–383 (1987).
63. Cooper, T. G. et al. World Health Organization reference values for human semen characteristics. *Hum. Reprod. Update* **16**, 231–245 (2010).
64. Ventimiglia, E. et al. When to perform karyotype analysis in infertile men? validation of the European association of urology guidelines with the proposal of a new predictive model. *Eur. Urol.* **70**, 920–923 (2016).
65. Wang, C. et al. Evolution of the WHO “Semen” processing manual from the first (1980) to the sixth edition (2021). *Fertil. Steril.* **117**, 237–245 (2022).
66. Gagliani, N., et al. Coexpression of CD49b and LAG-3 identifies human and mouse T regulatory type 1 cells. *Nat Med* (2013).
67. Mabbott, N. A., Baillie, J. K., Brown, H., Freeman, T. C. & Hume, D. A. An expression atlas of human primary cells: inference of gene function from coexpression networks. *BMC Genomics* **14**, 632 (2013).

## Acknowledgements

We thank the IRCCS San Raffaele Hospital Flow Cytometry facility (FRACTAL); Renato Ostuni, Marco Genua, and Nicoletta Caronni from San Raffaele Telethon Institute for GeneTherapy (SR-TIGET) for technical support in sample preparation for scRNA sequencing; Ivan Merelli and Matteo Barcellona from SR-TIGET Bioinformatic Core for kind advises for scRNAseq data analysis. We acknowledge Dana Kuefner for English editing of the manuscript. Supplementary Fig. 9a was created in BioRender (Santoni de Sio, F. (2025) <https://BioRender.com/j39n392>). A.S. and S.G. disclose support for the research of this work from the Italian Ministry of Health (RF-2019-12368847).

## Author contributions

G.A. performed research, interpreted data, and wrote the manuscript; G.G. performed bioinformatic analyzes and interpreted data; L.B. performed research and contributed to sample collection; M.R., S.C., F.B., F.N. managed patients and collected samples; E.P. and A.M.F. coordinated samples collection and biobanking; A.d'A. contributed to human

clinical data collection; F.R.S.d.S contributed to single-cell RNA sequencing; L.P. and E.P. performed and interpreted semen analyzes; E.V., M.A., and F.M. contributed to patient enrollment. A.S. and S.G. designed the study, interpreted data, coordinated, and supervised the whole research path, and wrote the manuscript.

### Competing interests

The authors declare no competing interests.

### Additional information

**Supplementary information** The online version contains supplementary material available at <https://doi.org/10.1038/s41467-025-56193-2>.

**Correspondence** and requests for materials should be addressed to Andrea Salonia or Silvia Gregori.

**Peer review information** *Nature Communications* thanks Daniel Oliveira Gomes and the other anonymous reviewer(s) for their contribution to the peer review of this work. A peer review file is available.

**Reprints and permissions information** is available at <http://www.nature.com/reprints>

**Publisher's note** Springer Nature remains neutral with regard to jurisdictional claims in published maps and institutional affiliations.

**Open Access** This article is licensed under a Creative Commons Attribution-NonCommercial-NoDerivatives 4.0 International License, which permits any non-commercial use, sharing, distribution and reproduction in any medium or format, as long as you give appropriate credit to the original author(s) and the source, provide a link to the Creative Commons licence, and indicate if you modified the licensed material. You do not have permission under this licence to share adapted material derived from this article or parts of it. The images or other third party material in this article are included in the article's Creative Commons licence, unless indicated otherwise in a credit line to the material. If material is not included in the article's Creative Commons licence and your intended use is not permitted by statutory regulation or exceeds the permitted use, you will need to obtain permission directly from the copyright holder. To view a copy of this licence, visit <http://creativecommons.org/licenses/by-nc-nd/4.0/>.

© The Author(s) 2025